SYNTHESIS OF PI CONJUGATED POLYMERS FOR USE IN PHOTOVOLTAIC AND ELECTROCHROMIC APPLICATIONS

A Thesis
Presented to
The Academic Faculty

by

James Joseph Deininger

In Partial Fulfillment
of the Requirements for the Degree
Chemistry Master of Science in the
School of Chemistry & Biochemistry

Georgia Institute of Technology
August 2015

SYNTHESIS OF PI CONJUGATED POLYMERS FOR USE IN PHOTOVOLTAIC AND ELECTROCHROMIC APPLICATIONS

Approved by:

Dr. John R. Reynolds, Advisor
School of Chemistry and Biochemistry
Georgia Institute of Technology

Dr. Elsa Reichmanis
School of Chemical and Biomolecular Engineering
Georgia Institute of Technology

Dr. Stefan France
School of Chemistry and Biochemistry
Georgia Institute of Technology

Date Approved: 05/07/2015

I would like to dedicate this thesis to my family and friends who have always been there with support and love – especially John and Nancy Deininger, Judy and Katlin Nicely, Nana, Papa, Malcolm Zellars, Joseph Lyske, Joel Aponte-Guzman, Hector Pacheco, George and Annie Poluse, Reza Mohammadpour, John Rolf, Noam Chomsky, and my best friend Danielle Deininger.

ACKNOWLEDGEMENTS

I would like to thank all those who have supported me throughout my graduate career, especially Dr. Reynolds and the members of the Reynolds group who have pushed me to grow intellectually.

TABLE OF CONTENTS

LIST OF TABLES

LIST OF FIGURES

LIST OF SCHEMES

LIST OF SYMBOLS AND ABBREVIATIONS

π	pi
^1H	Hydrogen Nuclear Magnetic Resonance
$\Delta\%T$	Change in Percent Transmission
k_{obs}	Observed Rate
DTS	Dithienosilole
DTG	Dithienogermole
OPVs	Organic Photovoltaics
OFETs	Organic Field Effect Transistors
OLEDs	Organic Light Emitting Diodes
NLOs	Non-Linear Optics
OECs	Organic Electrochromics
CPDT	Cyclopentadithiophene
BTD	2,1,3-benzodithiazole
TPD	N-octylthieno[3,4-c]pyrrole-4,6-dione
PCEs	Power Conversion Efficiencies
TLC	Thin Layer Chromotography
DTP	Dithienopyrrole
DHAP	Direct (hetero)arylation Polymerization
ECPS	Electrochromic polymers
PPM	Parts Per Million
OxP	Oxidative Polymerization
GRIM	Grignard metathesis
M_n	Normal Average Molecular Weight

ĐM	Polydispersity
DMAc	Dimethylacetamide
HCl	Hydrochloric acid
kDa	Kilodalton
MeOH	Methanol
DE	Dielectric Constant
DCM	Dichloromethane
GPC	Gel permeation Chromatography
GC-MS	Gas chromatography–mass spectrometry
2B3HT	2-bromo-3- hexylthiophene
Pd-scavenger	diethylammonium diethyldithiocar-bamate
18-crown-6	1,4,7,10,13,16-hexaoxacyclooctadecane
ICP-MS	Inductively Coupled Plasma Mass Spectrometry
NMP	N-Methylpyrrolidone
HMPA	Hexamethylphosphoramide
UV-Vis	Ultraviolet–Visible Spectroscopy
nm	Nanometers
ns	Nanoseconds
LED	Light-Emitting Diode
CMYK	Cyan, Magenta, Yellow, and Key (Black)
DP	Degree of Polymerization
THF	Tetrahydrofuran
ITO	Indium Tin Oxide

SUMMARY

Conjugated polymers are currently being used for a wide range of electronic applications. In this thesis, we studied two different synthetic approaches that lead to novel monomers and polymers that can be potentially used in electrochromic, or photovoltaic devices. Additionally, all the work described in this thesis has contributed to the scientific literature

The first approach described in this thesis is the utilization of olefin cross metathesis to create a family of dithienogermole (DTG) monomer derivatives in which synthetic control of the solubilizing side chains is achieved through an alkenyl building block. This alkenyl intermediate allows one to functionalize the DTG moiety though olefin cross metathesis to obtain a wide range of alkyl chain lengths and pendant functionalities on the polymer backbone. This work lead to the first example in the literature in which the synthesis of DTG moieties was not limited by the chain length of the solubilizing alkyl units. It provides a route that avoids the use of distillation for the purification the DTG monomer, allowing for the synthesis of a wide range of DTG derivatives that were previously unobtainable though the conventional synthetic methods.

Finally, in this thesis we also describe the work of the use of direct (hetero)arylation polymerizations (DHAP) as a means of obtaining 3,4-propylenedioxythiophene-based conjugated polymers for use in electrochromic applications. This synthetic method offers a rapid route to achieving polymers in high yields with simplified purification procedures and low residual metal content, as determined by inductive coupled plasma-mass spectrometry (ICP-MS). The studied polymers possess comparable electrochromic properties to those previously reported by the Reynolds group, implying that their switching ability from a colored to a transmissive state is independent of the residual metallic impurities.

CHAPTER 1

INTRODUCTION

1.1 Introduction to Conjugated Polymers

Conjugated polymers were first discovered in the 1970s by Heeger, MacDiarmid and Shirakawa who shared the Nobel Prize in chemistry in 2000 for their development of conjugated polymers[1]. By definition conjugated polymers consist of alternating single and double bonds along the carbon backbone of the polymer chain. Additionally, overlap of the carbon pi orbitals give rise to electron delocalization which in turn can make these polymers semiconducting or conducting materials – allowing a wide range of electronic applications.

The first conjugated polymer discovered was Polyacetylene which consists of alternating single and double bonds. Much work was done on this polymer in efforts to create a lightweight, flexible, and inexpensive plastic metal that could be utilized in commercial applications. It was discovered that when Polyacetylene was doped with an electron accepting (p-type) dopant such as bromine (Br_2) the conductivity of the overall system would increase. This increase in conductivity is explained by charge transfer between the electron donating polymer and electron accepting dopant.

Unfortunately, due to the film instability and synthetic challenges associated with Polyacetylene, no commercial applications currently utilize this polymer to date. However, the discoveries associated with polyacetlyne lead to extensive research into other polymeric systems such as polythiophene - which have shown promising commercial applications in organic light emitting diodes (OLEDs), organic field effect transistors (OFETs), organic photovoltaics (OPVs), Non-Linear Optics (NLOs), and organic electrochromics (OECs) to name a few.[2]

1.2 References

[1] "The Nobel Prize in Chemistry 2000." The Nobel Prize in Chemistry **2000**. N.p., n.d. Web. 09 Nov. 2014.

[2] Huaxing Zhou, Liqiang Yang, and Wei You *Macromolecules* **2012** 45 (2), 607-632

CHAPTER 2

EFFICIENT SYNTHESIS OF DITHIENOGERMOLE (DTG) DERIVATIVES VIA OLEFIN CROSS-METATHESIS

2.1 Introduction to Dithienosilole and Dithienogermole Donor Monomers and Polymers

Semiconducting copolymers containing dithienosilole (DTS) and dithienogermole (DTG) donors have attracted attention due to their utility in synthesizing molecules and polymers potentially useful in organic electronic applications, such as organic photovoltaics (OPVs) [1-6] and organic field effect transistors (OFETs).[7-10]

As shown in **Figure 2.1**, DTG is analogous in structure to cyclopentadithiophene (CPDT) and DTS where the carbon or silicon atom is substituted with germanium respectively.

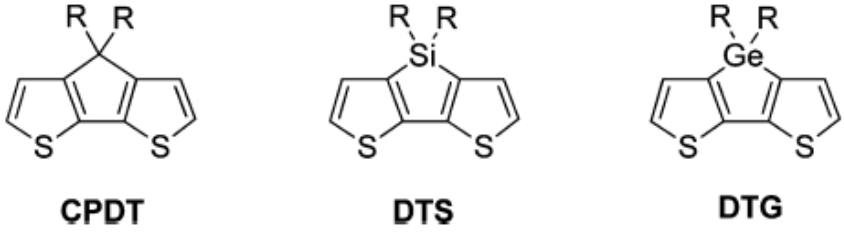

Figure 2.1 Structures of common fused systems used as donor moieties

In comparison with the C and Si atoms employed in CPDT or DTS, it has been reported that the bridging Ge atom in DTG[11-19] can result in an enhancement in intermolecular ordering, due to the long C-Ge bond lengths, moving the bulky side chains away from the planar heterocycle allowing stronger π-π stacking.[12] As shown in **Figure 2.2**, the copolymer between 4,4'-bis(2-ethylhexyl)dithieno-[3,2-b:2',3'-d]germole and 2,1,3-benzodithiazole (BTD) exhibits an FET mobility[18] up to 0.11 $cm^2 V^{-1} s^{-1}$ while the

copolymer with N-octylthieno[3,4-c]pyrrole-4,6-dione (TPD) has given solar cell AM 1.5 power conversion efficiencies (PCEs) up to 7.3%, higher than the corresponding DTS polymer.[12] Using an inverted cell morphology with interface control, DTG-TPD based polymer solar cells have been prepared with PCEs up to 8.5% (7.4% certified power conversion efficiency).[16]

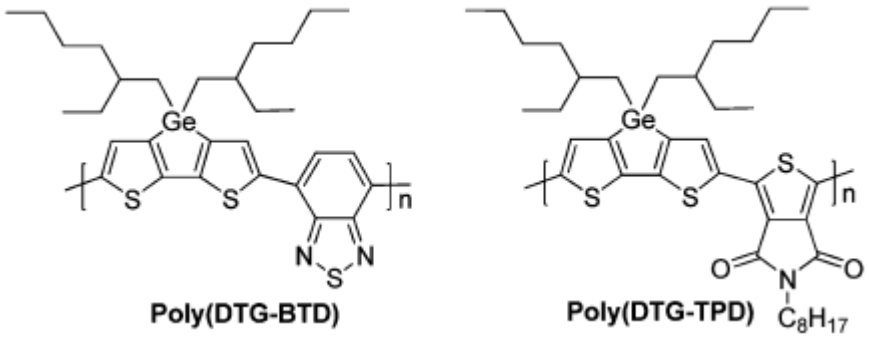

Figure 2.2 Polymer repeat unit structures for DTG-based materials with BTD and TPD acceptors employed in organic electronics and solar cells.

In order to prepare sufficiently soluble DTG-based polymers for effective processing, relatively long chain alkyl solubilizing groups are required on the bridging germanium atom. To date, the alkyl chains on DTG reported in the literature have been limited to 2-ethylhexyl, n-butyl, and methyl. One reason for this is due to the fact that while the dichlorodimethyl-, dichlorodiethyl-, and dibutyldichloro-germane intermediates are commercially available, others such as dichlorodiethylhexylgermane are not. Due to the synthetic complexity of preparing long chain dialkyldichlorogermane derivatives, it has been a challenge to synthesize multiple DTG derivatives.

The DTG core is generally constructed by reacting the 3,3'-dilithiated-2,2'-bithiophene **(2)** with a dialkyldichlorogermane **(1)** as shown in Scheme 2.1.[11-12,14] The longer alkyl derivatives, such as 2-ethylhexyl, are prepared from the reaction of $GePh_2Cl_2$ or $GeCl_4$ with the corresponding alkyl Grignard or alkyl lithiumreagents.[19]

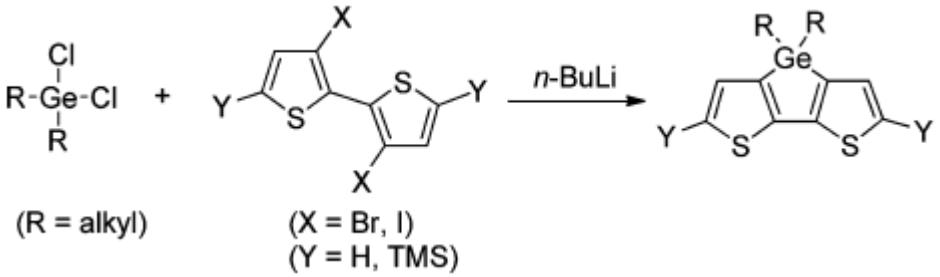

Scheme 2.1 General Synthetic Route for Construction of DTG Core

However, as the alkyl chain length becomes longer, the preparation of the organometallic reagents becomes difficult due to their lack of reactivity toward the magnesium or lithium metals.

Another challenge in the preparation of long chain dialkyldichlorogermanes lies in the purification, as they are generally isolated as oils by fractional vacuum distillation and are sensitive to moisture. As such, as the molecular weight of the compound increases, distillation becomes exceedingly difficult. Thus, in order to overcome these synthetic obstacles, we envisioned the synthesis of a single precursor compound, which can be easily manipulated in order to produce various DTG derivatives as illustrated in Scheme 2.2. This synthetic strategy eliminates the required isolation of a separate dialkyldichlorogermane for every new DTG derivative produced.

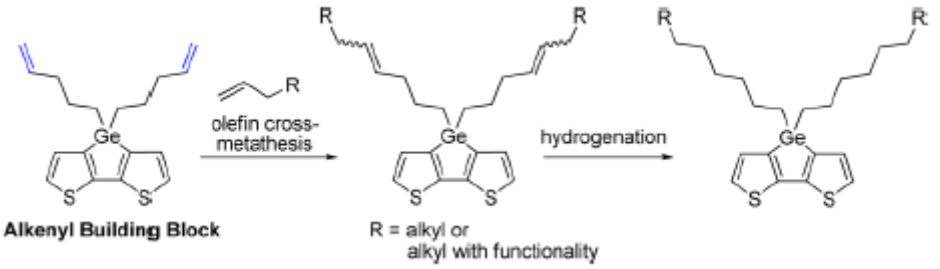

Scheme 2.2 Synthetic Strategy for Various DTG Derivatives from an Alkenyl Building Block Compound

2.2 Synthetic Results

In this study, DTG functionalized with terminal pentenyl chains on Ge (**Scheme 2.3**) was designed as a synthetic "building block" compound, as the terminal alkenyl group can be further functionalized via olefin cross-metathesis in order to install a variety of alkyl chains and further incorporate functionality including halides and esters.

For the preparation of 4, 4-pentenylmagnesiumbromide was prepared from magnesium and 4-pentenyl bromide and subsequently added to $GeCl_4$ by a slight modification of the published procedure, as illustrated by Scheme 2.3.[3b]

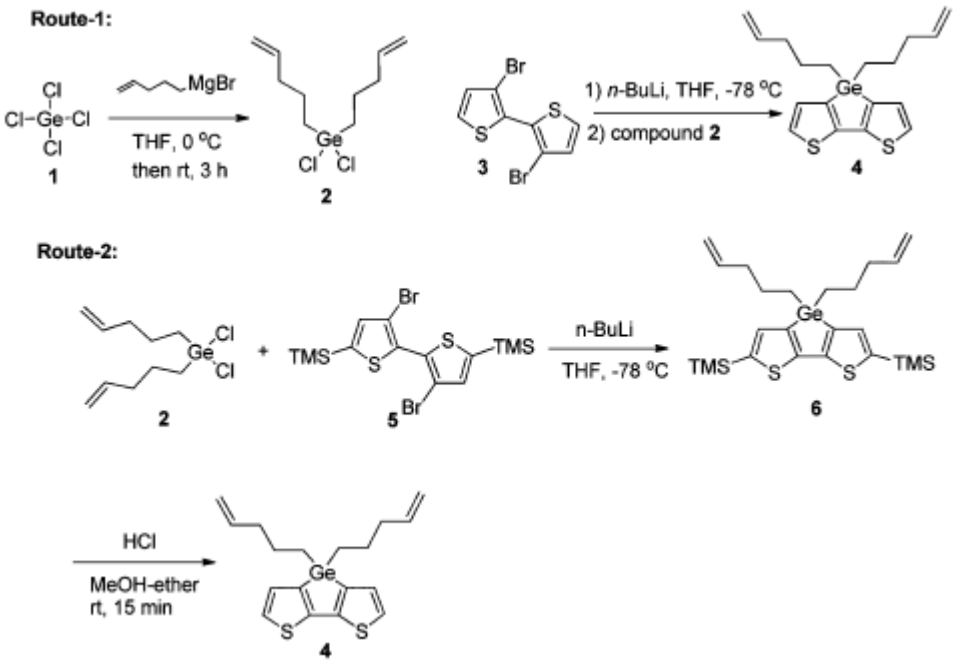

Scheme 2.3 Synthesis of 4,4'-Bis-(4-pentenyl)-dithieno-[3,2-*b*:2',3'-*d*]germole (**4**) as a Building Block Compound.

This reaction usually results in a mixture of several products (mono-, di-, and tri-substituted), yet the major fraction, dichloro-di-4-pentenylgemane (**2**), could be isolated by fractional distillation under reduced pressure in a 44 - 45% yield. To enhance product formation from starting reagents, the lowest boiling 4-pentenyltrichlorogermane fraction could be isolated and recycled for the preparation of **2**. Freshly distilled dichloro-di-4

pentenylgermane was added to 3,3'-dilithiated-2,2'-bithiophene prepared from 3,3'-dibromo-2,2'-bithiophene and n-BuLi at -78 ^{o}C to give 4,4'-bis-(4-pentenyl)-dithieno [3,2-b:2',3'-d]germole (**4**) in 52% yield (Route 1).

We subsequently explored the use of 2,2'-TMS functionalized bithiophene (**5**) in order to improve the yield by avoiding possible side reactions at the terminal 2,20-positions of bithiophene. The reaction of **2** with dilithiated **5** at -78 ^{o}C gave **6** in 65% yield. Subsequently, **6** was easily converted into **4** in 80% yield by stirring in 5% HCl solution in MeOH/ether for 10 min (Route 2). Although the latter route yielded **4** in an overall yield of 52%, it does require the additional step of TMS deprotection.

With **4** in hand, we explored the installation of extended alkyl chains and further functionalities by employing olefin cross-metathesis as shown in Scheme 2.4.[20] The competition between ring closing or cross-metathesis is known to be highly dependent upon the ratio of two alkenes employed.

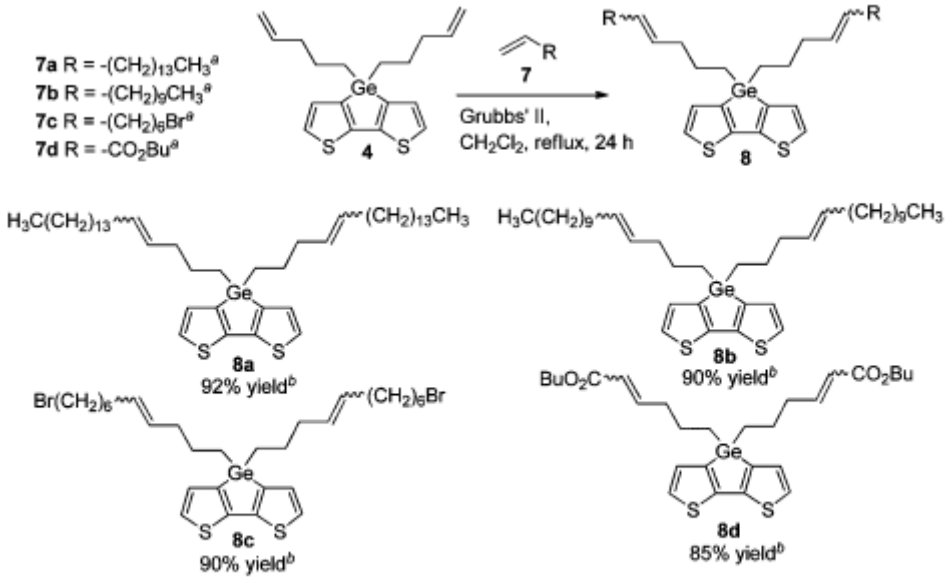

a. 16 equiv of alkenes were used.
b. Isolated yields reported as a mixture of *cis* and *trans* isomers.

Scheme 2.4 Synthesis of DTG Derivatives from Olefin Cross-Metathesis.

In order to minimize ring closure, or dimerization by self-metathesis and, thus, maximize the product by cross-metathesis, the ratio of **4** and **7** were closely examined and the optimal conditions were found to include use of an approximately16-fold excess of 7. The reaction of **4** with 16 equiv of 1-hexadecene (**7a**) under standard metathesis conditions gave **8a** in 92% yield. As expected, the products were composed of a mixture of *trans-trans*, *trans-cis*, and *cis-cis* isomers, which were inseparable by column chromatography on silica gel. The separation of these isomers is not necessary due to the fact that the double bonds are saturated in the next step. Similarly, the reaction of **4** with 1-dodecene (**7b**) yielded **8b** in 90%yield. In addition, cross-metathesis of **4** with alkenes having functionality, such as 8-bromooct-1-ene (**7c**) or butyl acrylate (**7d**), worked as well to give **8c** or **8d** in excellent yields.

Hydrogenation of the products obtained from cross-metathesis was investigated under several reaction conditions as shown in **Scheme 2.5**. Utilization of a hydrogen balloon in the presence of 5% or 10% Pd/C at ambient or elevated temperature was not successful. In these cases, the reactions gave a distribution of fully saturated, partially saturated, and unsaturated products as judged by TLC. Therefore, high pressure hydrogenation was carried out in the presence of Pd/Wilkinson's catalyst under various pressures and temperatures.[21] Optimal conditions for hydrogenation were achieved under 400 psi of hydrogen in the presence of 10 mol% Wilkinson's catalyst. Under these conditions, the reaction proceeded smoothly to afford fully saturated DTG derivatives in excellent yields as shown in **Scheme 2.5**.

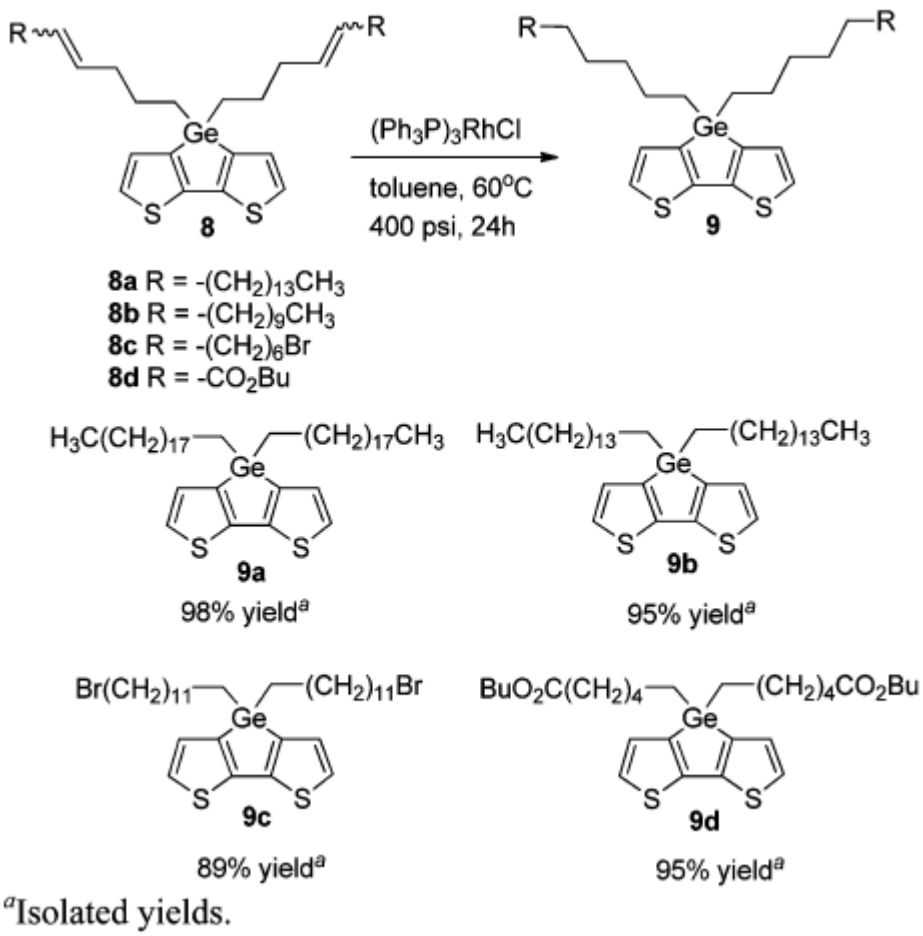

Scheme 2.5 Hydrogenation of **8** and Isolated Yields

In conclusion, we report a new efficient synthetic route that allows access to various DTG derivatives using olefin cross-metathesis as a key step. Terminally alkenylated DTG (**4**) serves as an easily accessed precursor for olefin cross-metathesis with various alkenes to yield unsaturated products with additional functionalities. Hydrogenation of these products afforded saturated DTG derivatives in excellent yields. The ability to access long alkyl chains, or variously functionalized DTGs, opens up new possibilities for synthesizing previously difficult to prepare donor materials for the organic electronic fields of OPV and OFETs, among others. The concepts reported herein can be extended to syntheses of many of the long chain and functional group modified

fused systems employed in organic electronics, such as the CPDT, DTS, and dithienopyrrole (DTP), along with organoboroles and organophospholes.

2.3 Synthetic Procedures and Characterization

General information: All reagents and starting materials were purchased from commercial sources and used without further purification, unless otherwise noted. The solvents were distilled and dried using known methods (W. L. F. Armarego, C. L. L. Chai, Purification of Laboratory Chemicals, 5th Edition, Elseier, 2003). All reactions were carried out under argon atmosphere unless otherwise mentioned.

Dichlorobis(4-pentyl)germane (2) Dry and clean magnesium turnings (5.3 g, 0.218 mol) were placed in a 500 mL two-neck round bottom flask and 200 mL of dry THF was charged under argon. 1,2-Dibromoethane (1.5 mL) and a small piece of I_2 crystal was added as an initiator. After stirring for about 20 min., the reaction became exothermic. Then, 5-bromo-1-pentene (32.5 g, 0.218 mol) was added dropwise via addition funnel for 1 hour while controlling the temperature. After the addition was completed the reaction was stirred at 60^{o}C for an additional 2 hours. The reaction mixture was cooled to room temperature, and the Grignard reagent was added into a dried addition funnel via a cannula under argon pressure. The Grignard reagent was then slowly added to a solution of $GeCl_4$ (23.4 g, 0.109 mol) in dry THF (250 mL) at 0 ^{o}C. The reaction was run for 4h and a large amount of white precipitate was observed. Hexanes (about 400 mL) were added and the mixture was stirred for additional 30 minutes. The mixture was carefully filtered under protection of moisture, and the solvent was removed by rotary evaporation. The residue was distilled (0.1-0.2 torr) to give three fractions, bp 65-85 ^{o}C (25- 30%), bp 86-95 ^{o}C (40-45%), bp 96-115 ^{o}C (3-5%), and the remaining residue. The middle bp fraction (bp 86-95 ^{o}C) consisted of a mixture of products that were utilized without

further purification. The first and third fractions were determined to be mono-alkyl substituted and tri-alkyl substituted germane respectively. The first fraction could be also utilized to produce the product by reacting with 1.0 equivalent of Grignard reagent. ^{1}H NMR (300 MHz, $CDCl_3$), δ: 5.70-5.83 (m, 2H), 4.93-5.08 (m, 4H), 2.05-2.22 (m, 4H), 1.68-1.72 (m, 8H).

General procedure for germole formation: To a solution of n-BuLi (13.6 mL of a 2.5M solution in hexane) in 250 mL diethyl ether at -78 ^{o}C was added dropwise a solution of 3, 3'dibromo-2,2'bithiophene (5.0g , 15.4 mmol) in THF (40 mL). The reaction mixture was stirred for 2.5 h at -78 ^{o}C and then a solution of dichlorobis(4-pentyl)germane (4.4g, 15.4 mmol) in diethyl ether (40 mL) was added dropwise. The reaction mixture was stirred for 1 h at -78 ^{o}C and then for overnight at room temperature. The reaction mixture was poured into 0.25 M aq. $NaHCO_3$ and extracted with hexanes (2 X 150 mL). The combined organic extracts were dried over $MgSO_4$, concentrated, and purified by chromatography on silica gel (neutralized by 4-5 drops of triethylamine) to give 3.0 g (52%) of 4 as a clear oil.

4,4'-bis-(4-pentenyl)-dithieno[3,2-b:2',3'-d]germole (4): Clear oil (52%) 1H NMR (300 MHz, $CDCl_3$) δ 7.19 (d, J=4.67 Hz, 2H), 7.03 (d, J=4.7 Hz, 2H), 5.65-5.80 (m, 2H), 4.84-4.95 (m, 4H), 2.02 (q, J=7.0 Hz, 4H), 1.52 (pent, J=7.6 Hz, 4H), 1.15-1.21 (m, 4H). 13C NMR (75 MHz, CDCl3) δ 147.1, 142.2, 138.4, 129.9, 125.1, 115.1, 36.9, 25.2, 14.1; HRMS (ESI-DART, M+H+) m/z calcd for $C_{18}H_{22}S_2Ge$ 377.0449, found 377.0464.

2,2'-bis-trimethylsilyl-4,4'-bis-(4-pentenyl)-dithieno[3,2-b:2',3'-d]germole (6): Clear oil (65%) 1H NMR (300 MHz, CDCl3) δ 7.10 (s, 1H), 5.65-5.80 (m, 2H), 4.84-4.95 (m, 4H), 2.04 (q, J=6.87 Hz, 4H), 1.53 (pent, J=7.45 Hz, 4H), 1.16 (m, 4H), 0.30 (s, 18H).

13C NMR (75 MHz, CDCl3) δ 147.1, 142.2, 138.4, 129.9, 125.1, 115.1, 36.9, 25.2, 14.1; HRMS (ESI-DART, M+H+) m/z calcd for $C_{24}H_{38}Si_2S_2Ge$ 521.1241, found 521.1249

General procedure for cross-olefin metathesis for 8a-8d: To a mixture of 2,2'-bis-trimethylsilyl-4,4'-bis-(4-pentenyl)-dithieno[3,2-b:2',3'-d]germole (1 equiv.) and alkene (16 eq.) in dichloromethane was added Grubb's (II) catalyst (6 mol% based on the germole) and the resulting mixture was heated at reflux temperature for 24 h under argon. The reaction mixture was cooled to room temperature and concentrated by rotary evaporation and the excess self-dimerized alkene was removed by selective precipitation by adding acetone. The residue was concentrated again and purified by column chromatography on silica gel using hexanes as eluent to give a mixture of cis-trans products. The mixture of products was used in the next reaction without the isolation of the cis and *trans* isomers. The experimental NMR details for compounds **8a-8d** are not provided since an isomeric mixture was obtained, followed by conversion into **9a-9d** which are fully characterized.

General procedure for hydrogenation for 9a-9d: Hydrogenation was performed using a 150 mL Parr high-pressure stainless reaction vessel equipped with a glass liner and a Teflon stirring bar. The unsaturated germole (1 mmol) was dissolved in dry toluene (20 mL) and added to the glass liner with Wilkinson's catalyst (10 mol %). The glass liner was placed into the bomb and then sealed. The Parr vessel was purged with 200 psi of hydrogen (H_2) three times and charged to 400 psi of hydrogen. The reaction mixture was stirred for 2 days at 50 ^{o}C. The crude mixture was concentrated by rotary evaporation and purified by column chromatography on silica gel using hexanes as an eluent to give the product.

4,4'-bis-(nonadecanyl)-dithieno[3,2-b:2',3'-d]germole (9a): white solid (98%)1H NMR (300 MHz, CDCl3) δ 7.18 (d, J=4.68 Hz, 2H), 7.02 (d, J=4.68 Hz, 2H), 1.08-1.48 (m, 72H), 0.85 (t, J=6.86 Hz, 6H); 13C NMR (75 MHz, CDCl3) δ 146.9, 142.8, 129.9, 124.9, 32.9, 32.1 29.9-29.4 (a bundle of peaks), 25.7, 22.9, 14.6, 14.4; HRMS (ESI-DART, M+H+) m/z calcd for $C_{46}H_{82}S_2Ge$ 773.5152, found 773.5171

4,4'-bis-(pentadecanyl)-dithieno[3,2-b:2',3'-d]germole (9b): clear oil (95%)1H NMR (300 MHz, CDCl3) δ 7.18 (d, J=4.67 Hz, 2H), 7.02 (d, J=4.67 Hz, 2H), 1.10-1.45 (m, 56H), 0.85 (t, J=6.86 Hz, 6H); 13C NMR (75 MHz, CDCl3) δ 146.9, 142.8, 129.9, 124.9, 33.0, 32.1 29.9-29.4 (a bundle of peaks), 25.8, 22.9, 14.6, 14.3; HRMS (ESI-DART, M+H+) m/z calcd for $C_{38}H_{66}S_2Ge$ 661.3898, found 661.3905

4,4'-bis-(butyl hexan-6-oatyl)-dithieno[3,2-b:2',3'-d]germole (9c): clear oil (89%) 1H NMR (300 MHz, CDCl3) δ 7.22 (d, J=4.67 Hz, 2H), 7.04 (d, J=4.67 Hz, 2H), 4.04 (t, J=6.73 Hz, 4H), 2.21 (t, J=7.45 Hz, 4H), 1.15-1.65 (m, 24H), 0.92 (t, J=7.3 Hz, 6H); 13C NMR (75 MHz, CDCl3) δ 173.7, 146.8, 142.0, 129.6, 124.8, 64.1, 34.1, 32.1, 30.6, 25.1, 24.4, 19.1, 14.1, 13.7; HRMS (ESI-DART, M+H+) m/z calcd for $C_{28}H_{42}O_4S_2Ge$ 581.1829, found 581.1829

4,4'-bis-(11-bromoundecanyl)-dithieno[3,2-b:2',3'-d]germole (9d): clear oil (95%) 1H NMR (300 MHz, CDCl3) δ 7.19 (d, J=4.68 Hz, 2H), 7.01 (d, J=4.68 Hz, 2H), 3.37 (t, J=6.86 Hz, 4H), 1.81 (pent, J=7.31 Hz, 4H), 1.10-1.45 (m, 32H); 13C NMR (75 MHz, CDCl3) δ 146.9, 142.7, 129.9, 124.9, 34.3, 33.0, 32.9, 29.6 (2C), 29.3 (2C), 28.9, 28.3, 25.7, 14.6; HRMS (ESI-DART, M+H+) m/z calcd for $C_{30}H_{48}Br_2S_2Ge$ 707.0837, found 707.0848

2.4 NMR Spectra & HRMS (ESI-DART, M+H+) m/z of Significant compounds

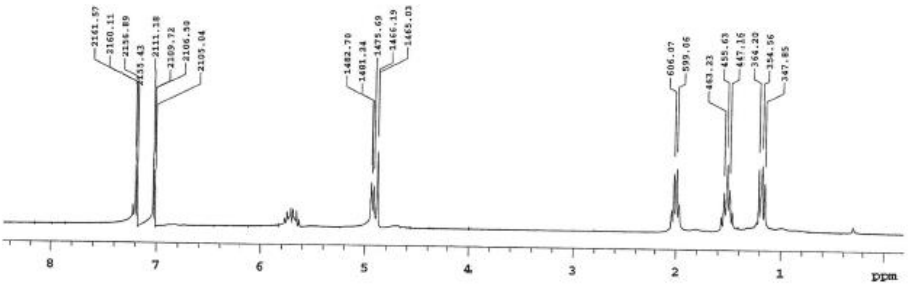

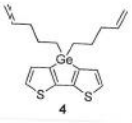

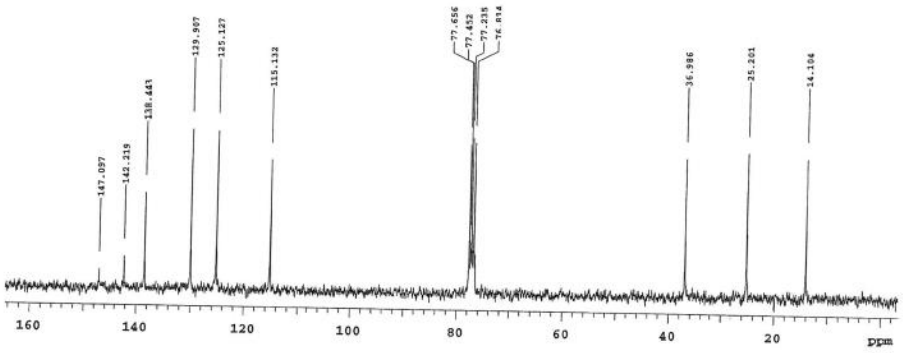

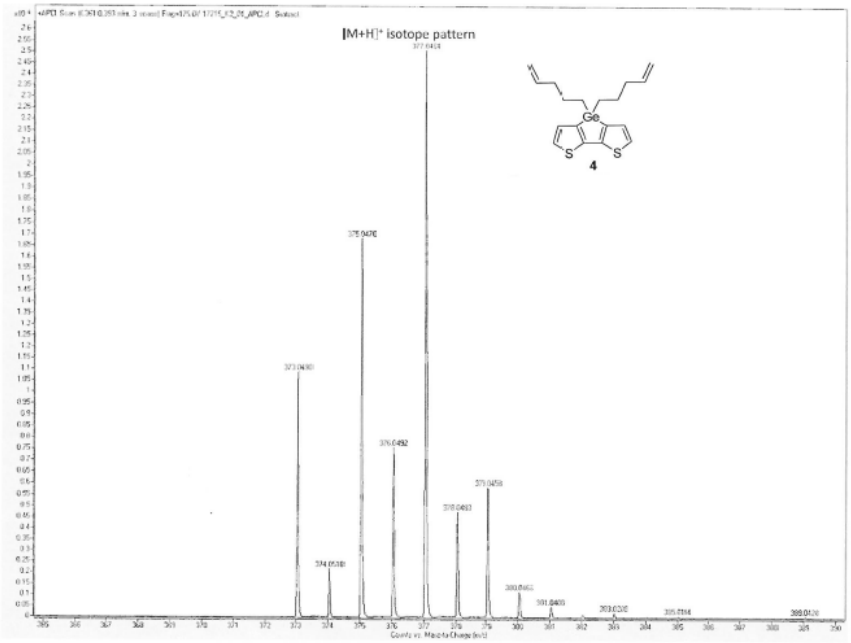
[M+H]+ isotope pattern
Ge
S
S
4

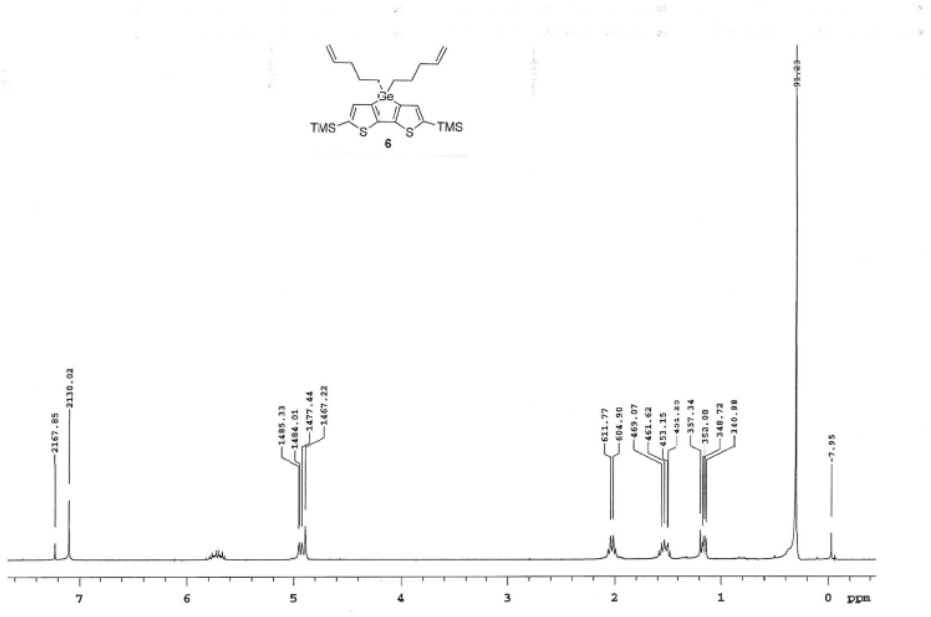
Ge
TMS
S
S
TMS
6
2167.85
2130.02
1489.33
1484.01
1477.44
1467.22
611.77
604.90
469.07
461.62
453.15
357.34
352.08
348.72
340.98
7.95
7
6
5
4
3
2
1
0
ppm

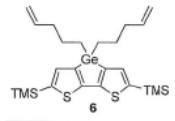
Ge
TMS
S
S
TMS

6

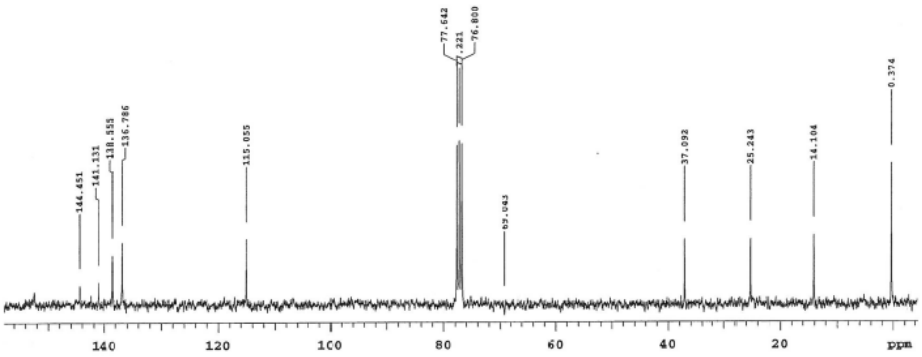
144.451
141.131
138.555
136.786
115.055
77.642
77.321
76.800
63.043
37.092
25.243
14.104
0.374
140
120
100
80
60
40
20
ppm

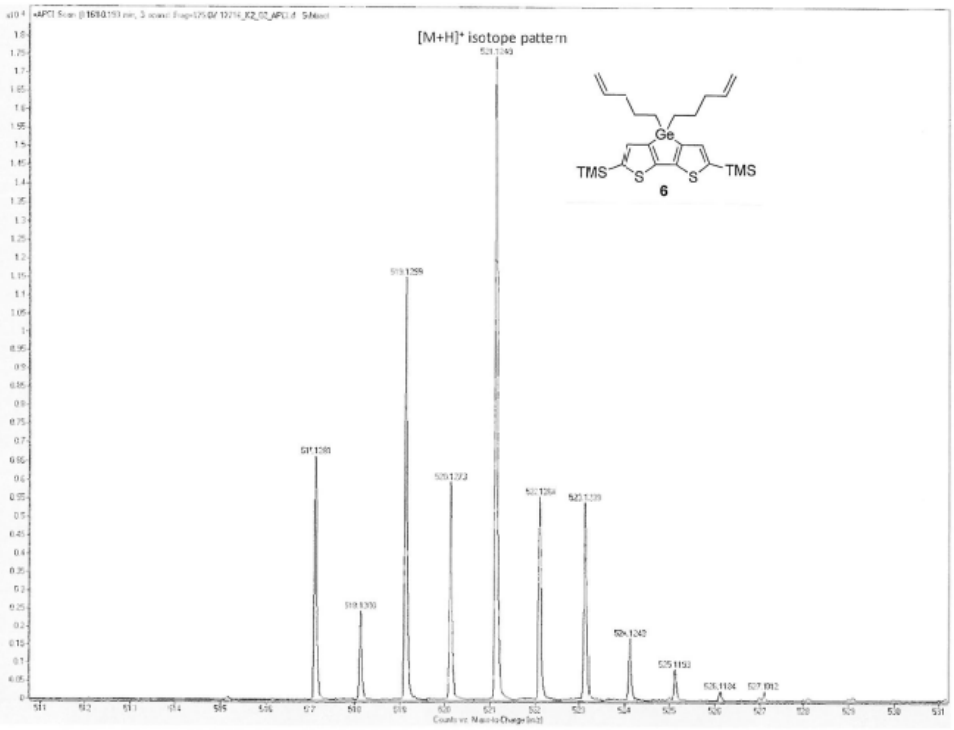
[M+H]+ isotope pattern
Ge
TMS
S
S
TMS
6

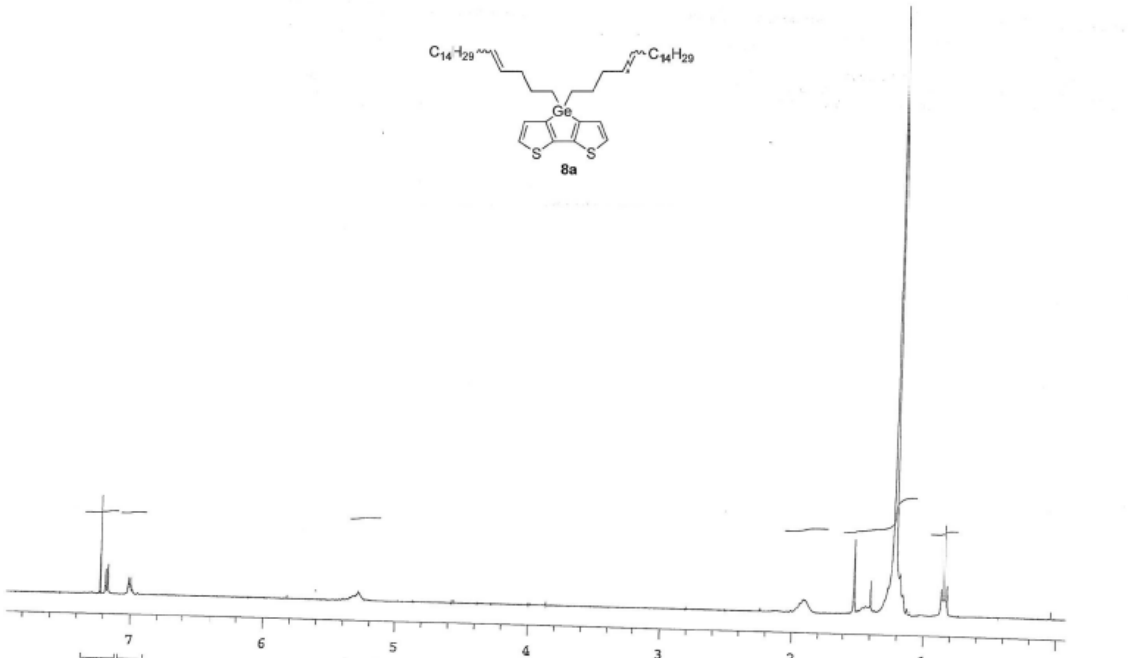
$C_{14}H_{29}$
$C_{14}H_{29}$
Ge
S
S
8a
7
6
5
4
3

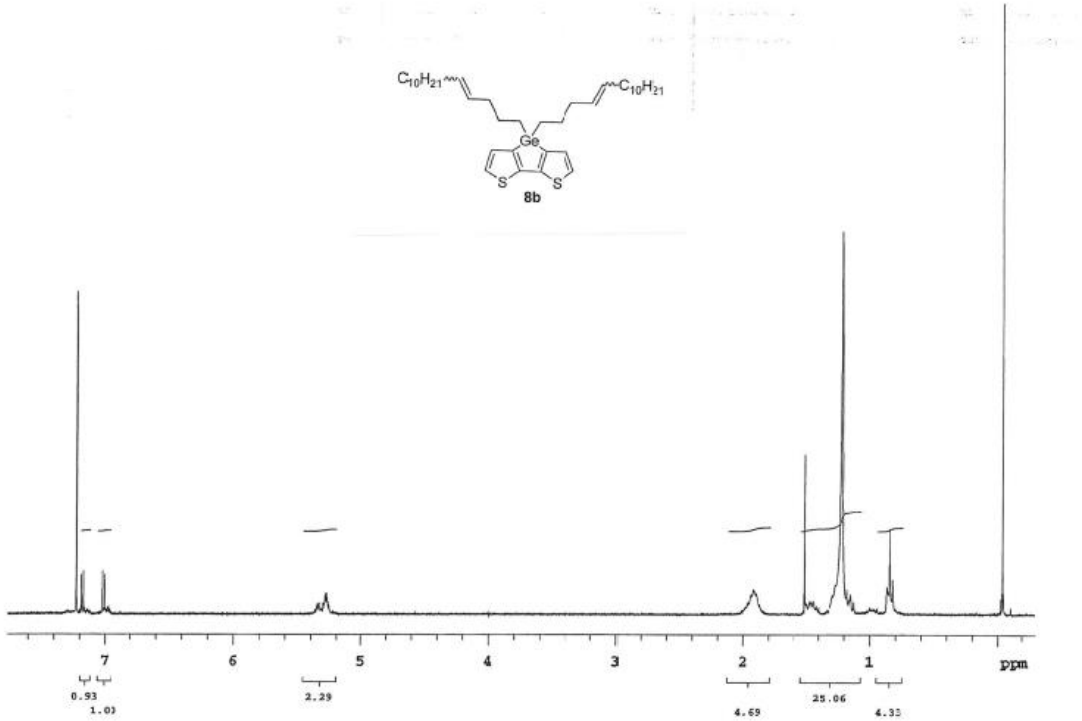
$C_{10}H_{21}$
$C_{10}H_{21}$
Ge
S
S
8b
7
6
5
4
3
2
1
ppm
0.93
1.03
2.29
4.69
25.06
4.33

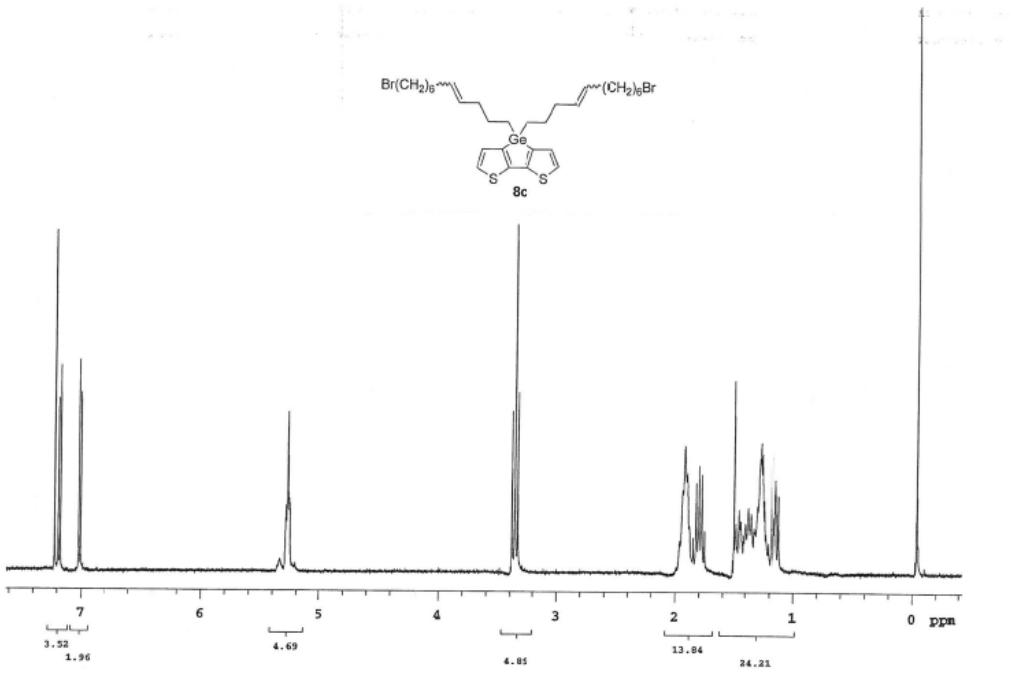
Br(CH2)6
(CH2)6Br
Ge
S
S
8c
7
6
5
4
3
2
1
0 ppm
3.52
1.96
4.69
4.85
13.84
24.21

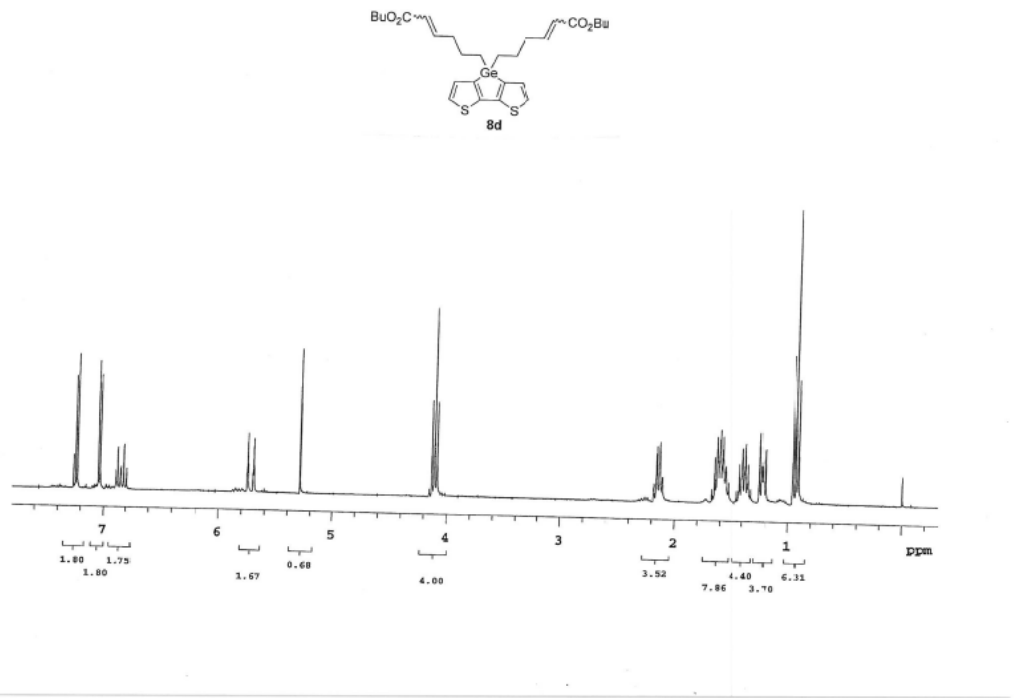
BuO2C
CO2Bu
Ge
S
S
8d
7
6
5
4
3
2
1
ppm
1.80
1.80
1.75
1.67
0.68
4.00
3.52
7.86
4.40
3.70
6.31

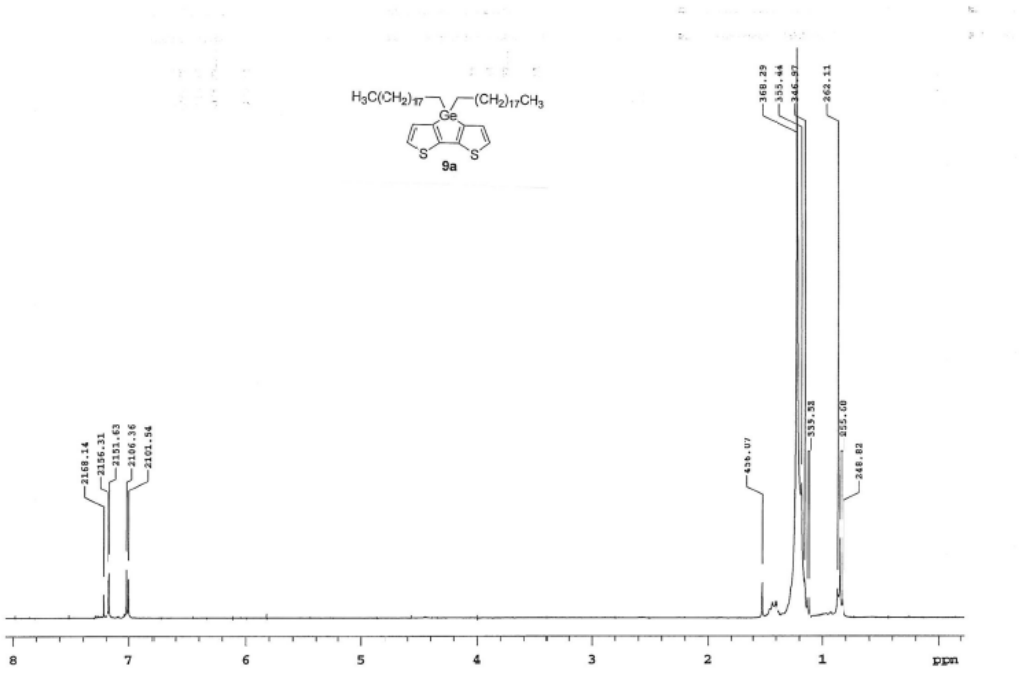
H3C(CH2)17
(CH2)17CH3
Ge
S
S
9a
2160.14
2156.31
2153.63
2106.36
2101.54
438.07
360.29
355.44
346.87
335.58
262.11
255.60
248.82
8
7
6
5
4
3
2
1
ppm

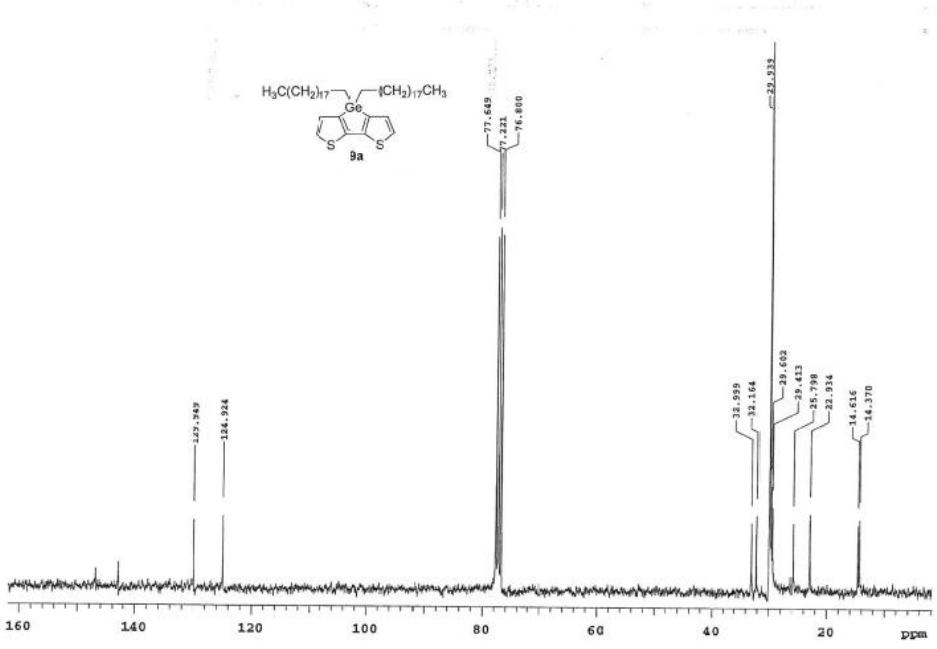
H3C(CH2)17
(CH2)17CH3
Ge
S
S
9a
77.649
77.321
76.800
32.533
32.999
32.164
29.602
29.413
25.798
22.934
14.616
14.370
129.949
124.924
160
140
120
100
80
60
40
20
ppm

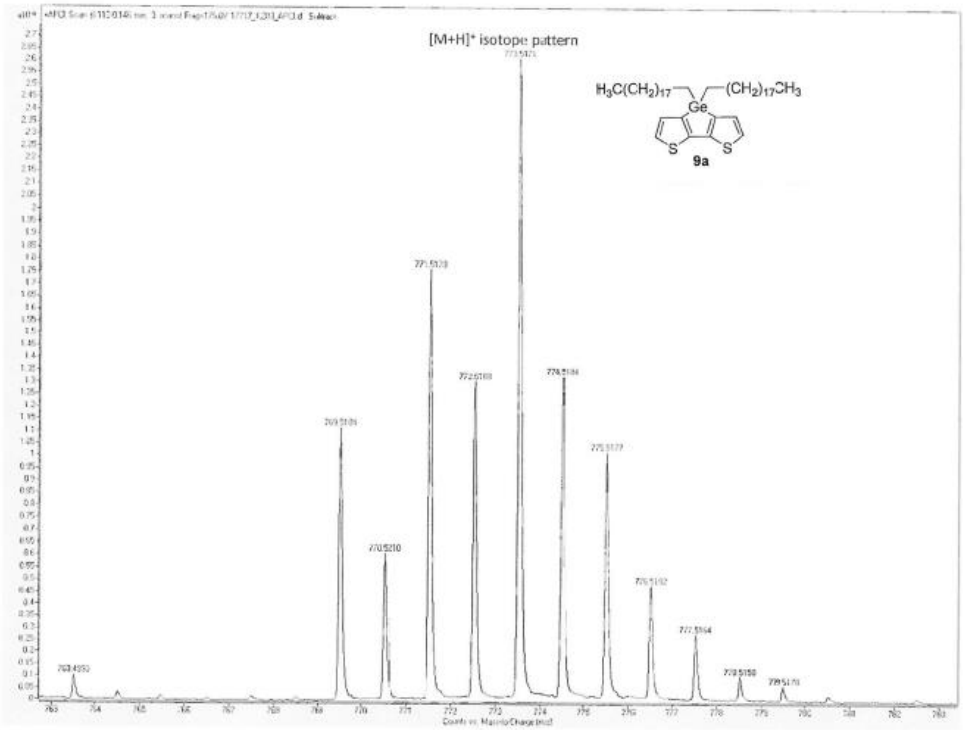
[M+H]+ isotope pattern
H3C(CH2)17
(CH2)17CH3
Ge
S
S
9a

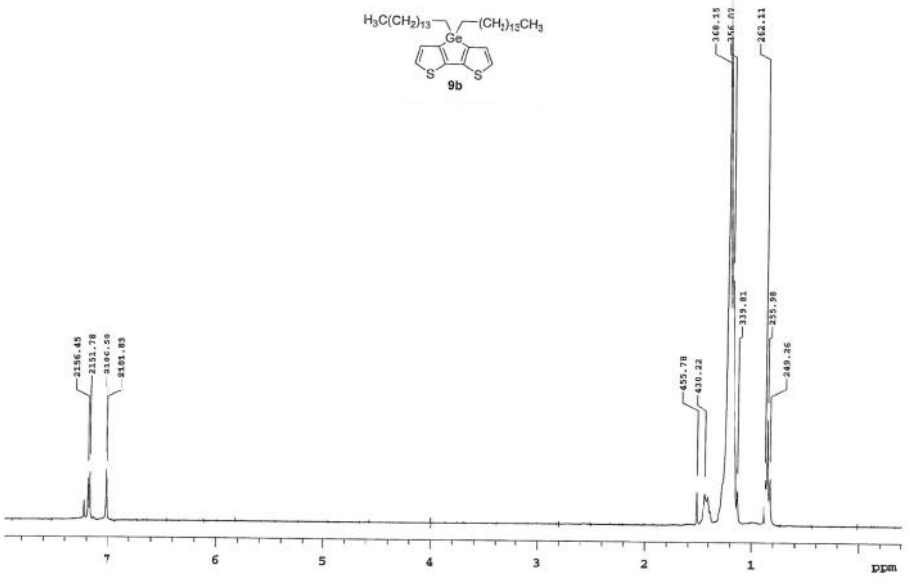
H3C(CH2)13
(CH2)13CH3
Ge
S
S
9b
2156.45
2151.78
2106.50
2101.83
455.78
430.22
368.15
366.09
339.81
261.11
255.98
249.26
7
6
5
4
3
2
1
ppm

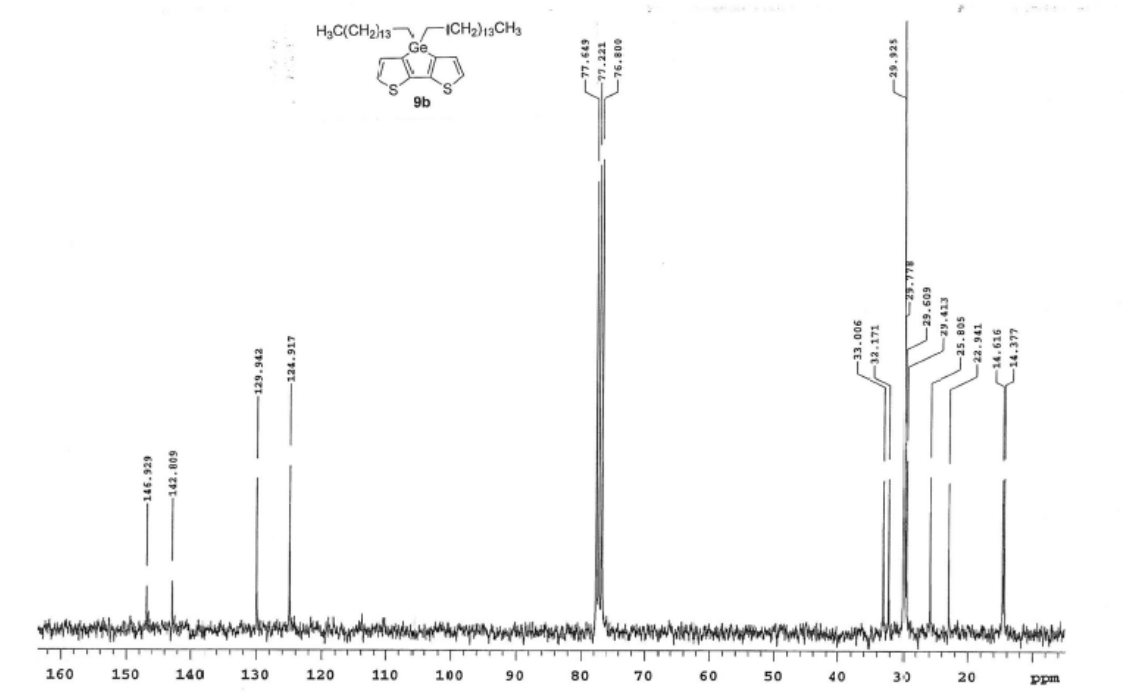
H3C(CH2)13
(CH2)13CH3
Ge
S
S
9b
77.649
77.221
76.800
29.925
29.778
29.609
29.413
25.805
22.941
14.616
14.377
33.006
32.171
129.942
124.917
146.929
142.809
160
150
140
130
120
110
100
90
80
70
60
50
40
30
20
ppm

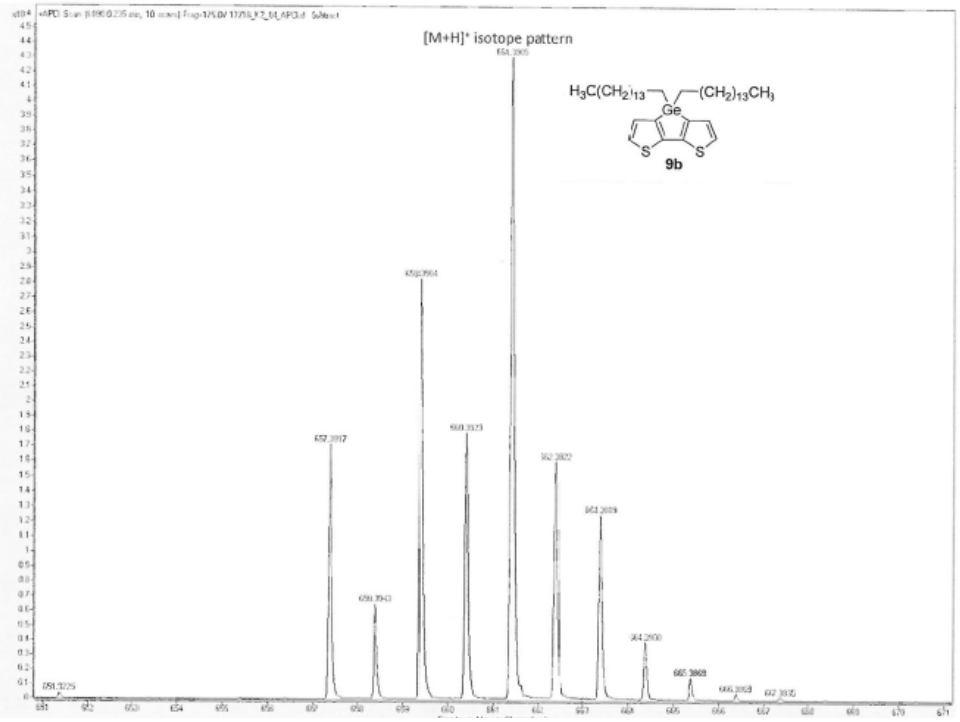
[M+H]+ isotope pattern
H3C(CH2)13
(CH2)13CH3
Ge
S
S
9b

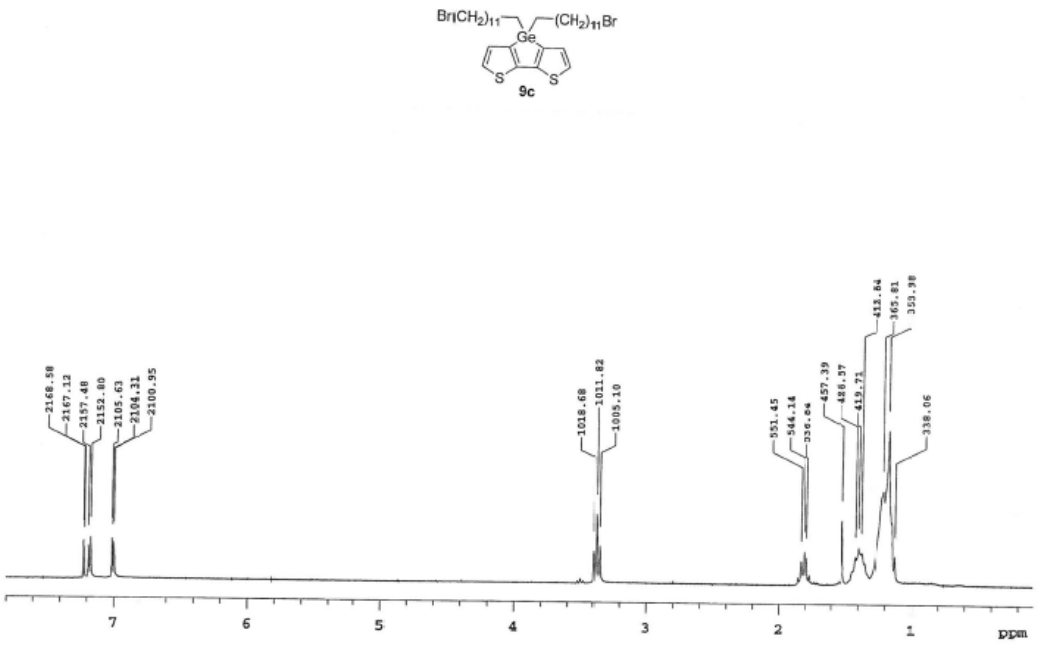
Br(CH2)11
(CH2)11Br
Ge
S
S
9c
2168.58
2167.12
2157.48
2152.80
2105.63
2104.31
2100.95
1018.68
1011.82
1005.10
551.45
544.34
536.64
457.39
448.57
419.71
413.64
365.81
359.98
338.06
7
6
5
4
3
2
1
ppm

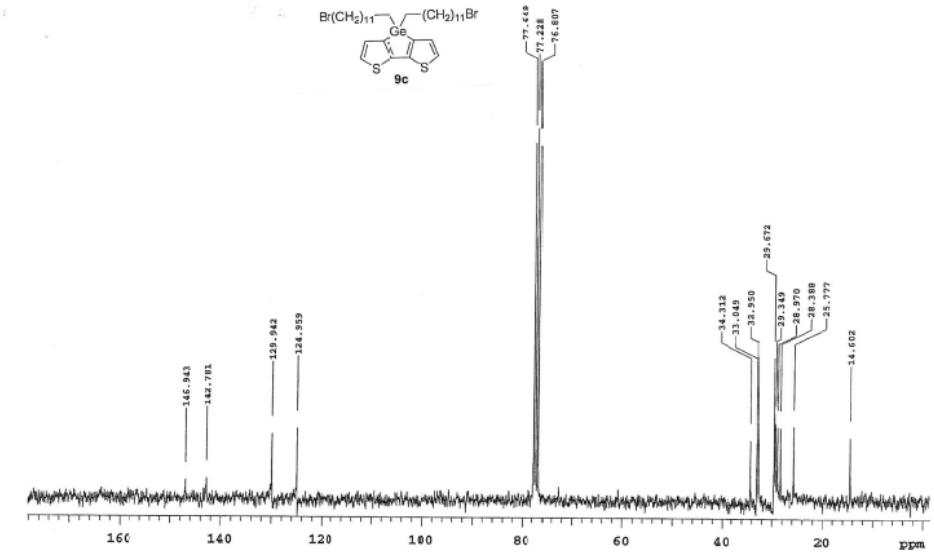
Br(CH2)11
(CH2)11Br
Ge
S
S
9c
77.449
77.228
76.807
146.943
142.781
130.942
124.959
39.672
34.312
33.049
32.950
29.349
28.970
28.388
25.777
14.602
160
140
120
100
80
60
40
20
ppm

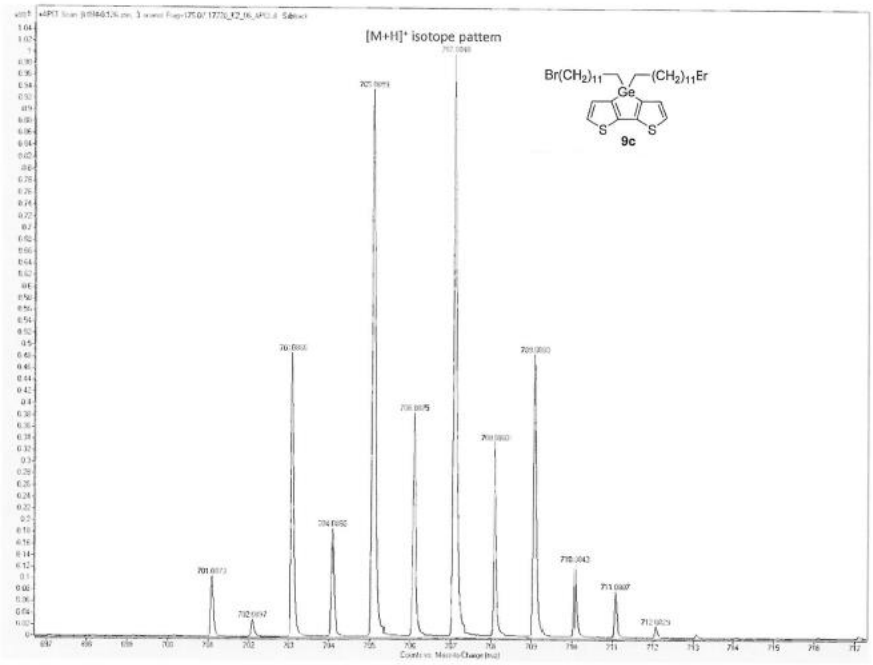
[M+H]+ isotope pattern
Br(CH2)11
(CH2)11Er
Ge
S
S
9c

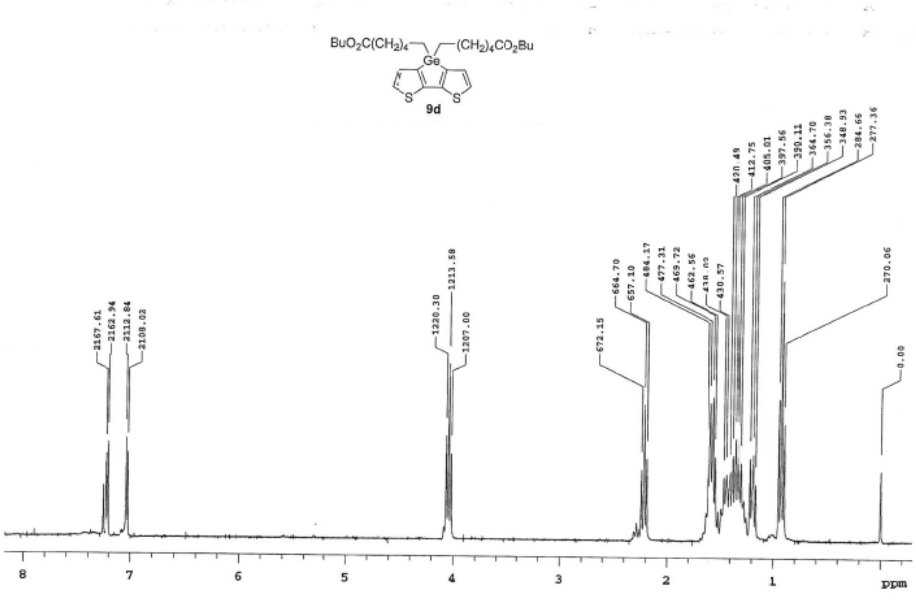
BuO2C(CH2)4
(CH2)4CO2Bu
Ge
S
S
9d
2167.61
2162.94
2112.84
2108.02
1220.30
1213.58
1207.00
672.15
664.70
657.10
484.17
477.31
469.72
462.56
430.57
430.49
412.75
405.01
397.56
390.11
364.70
356.38
348.93
284.66
277.36
270.06
0.00
8
7
6
5
4
3
2
1
ppm

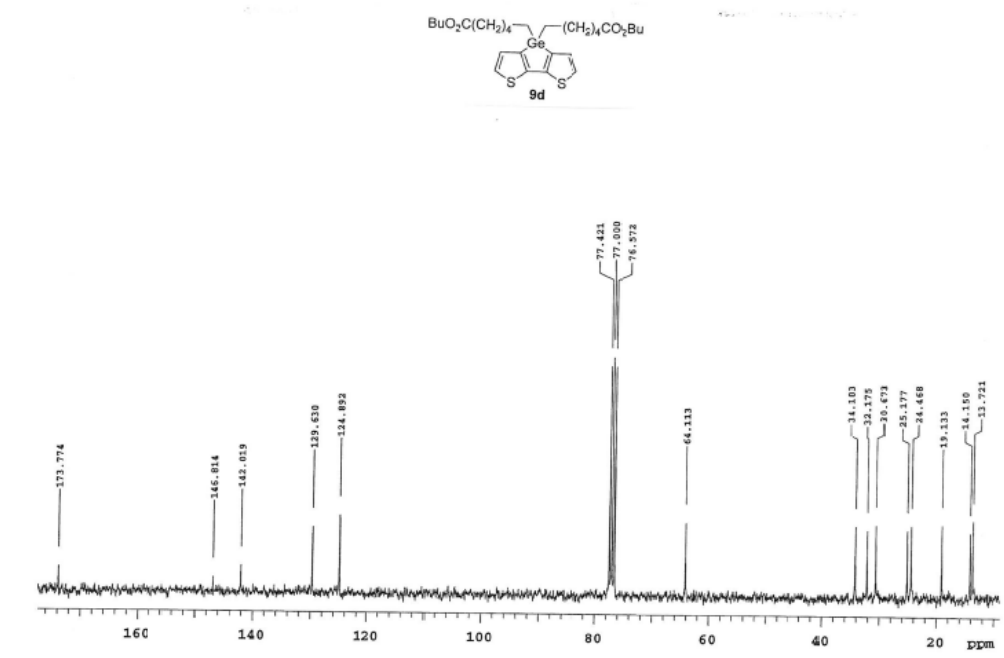
BuO2C(CH2)4
(CH2)4CO2Bu
Ge
S
S
9d
77.421
77.000
76.572
173.774
146.814
142.059
129.630
124.892
64.133
34.103
32.175
30.473
25.177
24.468
19.133
14.150
13.721
160
140
120
100
80
60
40
20
ppm

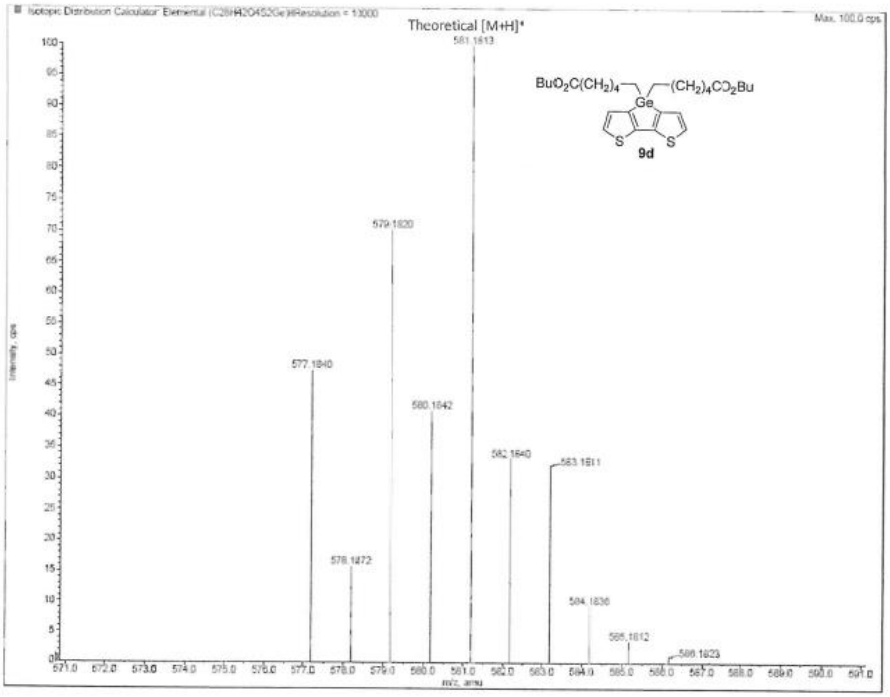
Isotopic Distribution Calculator Elemental (C28H42O4S2Ge)#Resolution = 10000
Theoretical [M+H]+
Max. 100.0 cps.
581.1613
BuO2C(CH2)4
(CH2)4CO2Bu
Ge
S
S
9d
579.1620
577.1640
580.1642
582.1640
583.1611
578.1472
584.1636
585.1612
586.1623
Intensity, cps
m/z, amu

2.5 References

[1] Gunes, S.; Neugebauer, H.; Sariciftci, N. S. *Chem. Rev.* **2007**, 107, 1324–1338.

[2] Thompson, B. C.; Fr_echet, J. M. J. *Angew. Chem., Int. Ed.* **2008**, 47, 58–77.

[3] Kippelen, B.; Br_edas, J.-L. *Energy Environ. Sci.* **2009**, 2, 251–261.

[4)] Dennler, G.; Scharber, M. C.; Brabec, C. J. *Adv. Mater.* **2009**, 21, 1323–1338.

[5] Boudreault, P.-L. T.; Najari, A.; Leclerc, *M. Chem. Mater.* **2011**, 23, 456–469.

[6] Zhou, H.; Yang, L.; You, W. *Macromolecules* **2012**, 45, 607–632.

[7] Sirringhaus, H.; Tessler, N.; Friend, R. H. *Science* **1998**, 281, 1741–1744.

[8] Forrest, S. R. *Nature* **2004**, 428, 911–918.

[9] Locklin, J.; Roberts, M.; Mannsfeld, S.; Bao, Z. *Polym. Rev*. **2006**, 46, 79–101.

[10] Zaumseil, J.; Sirringhaus, H. *Chem. Rev*. **2007**, 107, 1296–1323.

[11] Ohshita, J.; Hwang, Y.-M.; Mizumo, T.; Yoshida, H.; Ooyama, Y.; Harima, Y.; Kunugi, Y. *Organometallics* **2011**, 30, 3233–3236.

[12] Amb, C. M.; Chen, S.; Graham, K. R.; Subbiah, J.; Small, C. E.; So, F.; Reynolds, J. R. *J. Am. Chem. Soc*. **2011**, 133, 10062–10065.

[13] Hwang, Y.-M.; Ohshita, J.; Harima, Y.; Mizumo, T.; Ooyama, Y.; Morihara, Y.; Izawa, T.; Sugioka, T.; Fujita, A. *Polymer* **2011**, 52, 3912–3916.

[14] Gendron, D.; Morin, P.-O.; Berrouard, P.; Allard, N.; Aı¨ch, B. R.; Garon, C. N.; Tao, Y.; Leclerc,M. *Macromolecules* **2011**, 44, 7188–7193.

[15] Fei, Z.; Kim, J. S.; Smith, J.; Domingo, E. B.; Anthopoulos, T. D.; Stingelin, N.; Watkins, S. E.; Kim, J.-S.; Heeney, M. *J. Mater. Chem.* **2011**, 21, 16257–16263.

[16] Small, C. E.; Chen, S.; Subbiah, J.; Amb, C. M.; Tsang, S.-W.; Lai, T.-H.; Reynolds, J. R.; So, F. *Nat. Photonics* **2012**, 6, 115–120.

[17] Fei, Z.; Kim, Y.; Smith, J.; Domingo, E. B.; Stingelin, N.; McLachlan, M. A.; Song, K.; Anthopoulos, T. D.; Heeney, M. *Macromolecules* **2012**, 45, 735–742.

[18] Kim, J. S.; Fei, Z.; James, D. T.; Heeney, M.; Kim, J.-S. *J. Mater. Chem.* **2012**, 22, 9975–9982.

[19] Nicolas, A.; Aı¨ch, R. B.; Gendron, D.; Boudreault, P.-L. T.; Tessier, C.; Alem, S.; Tse, S.-C.; Tao, Y.; Leclerc, M. *Macromolecules* **2010**, 43 (5), 2328–2333.

[20] Chatterjee, A. K.; Choi, T.-L.; Sanders, D. P.; Grubbs, R. H. *J. Am. Chem. Soc.* **2003**, 125, 11360–11370.

[21] Sworen, J. C.; Wagener, K. B. *Macromolecules* **2007**, 40, 4414–4423.

CHAPTER 3

DIRECT (HETERO)ARYLATION POLYMERIZATION: AN EFFECTIVE ROUTE TO 3,4-PROPYLENEDIOXYTHIOPHENE-BASED POLYMERS WITH LOW RESIDUAL METAL CONTENT

3.1 INTRODUCTION TO METAL CATALYZED POLYMERIZATIONS

The organic electronics community has benefited tremendously from the development of palladium catalyzed cross-coupling reactions[1], which offer facile access to a wide range of chemical structures that would otherwise be challenging to achieve.[2] This capability has enabled structure-property relationship studies that provide design parameters for useful organic materials. The unique process ability of organic materials renders these attractive, since the replacement of inorganic semiconductors with organic surrogates might help to decrease device fabrication costs.[3]

Furthermore, considerable research efforts have been devoted to the simplification of these reactions. The success of Heck protocols[4] for the coupling of vinyl termini to halogenated arenes has generated a large amount of work that, building upon the work of Ullmann[5] and Goldberg[6], led to the discovery of "activated" C (sp2)-H bonds in aromatic systems that react in similar fashion.[7] The Pd-catalyzed direct arylation of (pseudo)halides or their derivatives has been rapidly developing through the years to the point where minute amounts of undesired side products are generated upon coupling completion. While the mechanistic details of the Pd insertion to the activated C-H bond are yet to be fully understood [8-11], successful protocols have been developed for the coupling of thienyl-based molecules to a wide variety of organic halides.[12,13] Once it was reported that this dehydrogenative cross-coupling takes place at fast rates under

phosphine-free conditions[14], many groups[15-21] successfully transposed this improved methodology for the synthesis of thiophene-based conjugated polymers – hence its name direct (hetero)arylation polymerization (DHAP).

Compared to the standard Suzuki and Stille polymerizations, DHAP simplifies the purification procedures for the obtained conjugated polymers thus reducing overall costs.[25] Furthermore, the absence of phosphine in the reaction mixture avoids its incorporation into the polymer backbone[26,27], which is often the reason why residual phosphine or phosphorus is hard to remove from the polymer during the purification stage. The residual contaminants left in conjugated polymers are often associated with poor performances when these are utilized as active components for electronic devices.[28-33] Such impurities (Sn, Pd, and Br based) can act as charge trapping sites thus hampering efficient charge transport. Therefore, it is important to understand the type and quantity of residual impurities of various polymerization protocols due to the potential high impact that these may have in their final application.

3.2 RESULTS

As an attempt to understand this, we have applied DHAP for the synthesis of 3,4-propylenedioxythiophene-based electrochromic polymers (ECPs). We have found that the DHAP is appealing for the preparation of polymers with low residual metal content (10-100 ppm) given the simplified purification process. Additionally, these polymers display vibrant colors and electrochromic properties comparable to those previously reported by us using other transition-metal based procedures.[34-35]

We investigated the impact of residual impurities in the color purity and transparency upon oxidation of our ECPs with the intent to reduce fabrication costs and

increase performance. For this, the synthesis of the homopolymer ECP-Magenta served as an initial standard to examine the residual metal content generated from common routes, illustrated in Scheme 3.1, such as oxidative polymerization (OxP)[36,37], Grignard metathesis (GRIM)[38,39], or Pd-catalyzed cross couplings. OxP yields ECP-Magenta with molecular weights (M_n) of 30 kDa on average, yet large amounts of $FeCl_3$ (≥4 eq) are necessary to achieve these weights. [38,39] This approach creates difficulties during the purification stage through the disposal of large amounts of residual Fe/Fe(II) composites. In comparison, Grignard metathesis (GRIM) polymerization also provides polymers with high molecular weights (M_n = 10-48 kDa), although the removal of impurities via Soxhlet extraction requires multiple days.

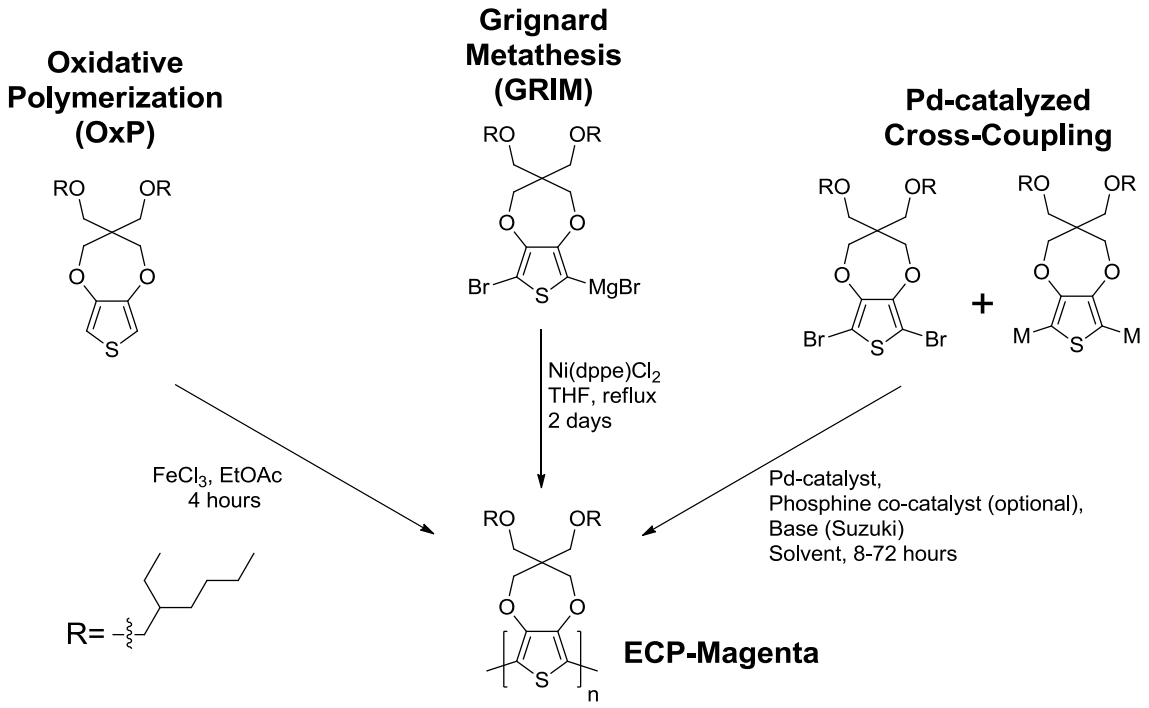

Scheme 3.1: Synthetic routes studied for the generation of ECP-Magenta.

We have noticed after using slightly modified conditions to those reported by Kanbara, [16] illustrated in Scheme 3.2 as direct (hetero)arylation polymerization (DHAP),

that there is a compromise between processing time and atom economy for the synthesis and purification of ECP-Magenta which is completed in less than one day.

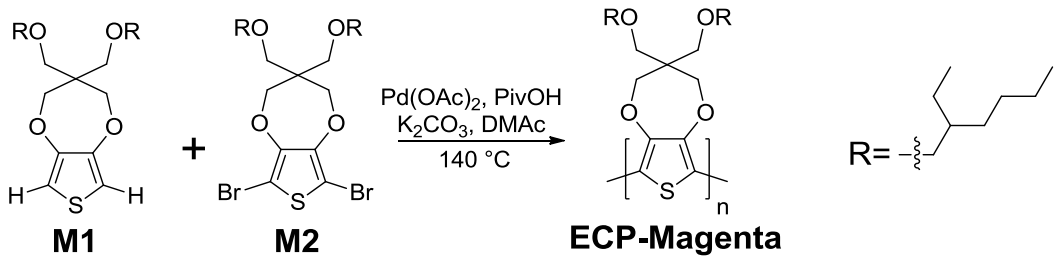

Scheme 3.2: Synthesis of ECP-Magenta via DHAP.

We have found that the role of the temperature is important; the reaction is slower within the 80-100 °C range than at 140 °C where the transformations occur at fast rates without any noticeable decomposition. Our observations are in line with previous reports of Yu et al.[19] where almost identical substrates (in their case, R = n-C_6H_{13}) fail to react in DMAc at 100 °C. This is contrary to our observations for numerous polymerizations. The initial characterization analysis was performed after precipitating the polymer in a 1:1 MeOH/1 N aqueous HCl solution with vigorous stirring followed by filtration and washing with copious amount of water (until AgCl test is negative) and then MeOH. The utilization of this procedure resulted in high yielding (80-90 %) polymers with $M_n \geq 10$ kDa against polystyrene standards and relatively small dispersities (ĐM ~ 1.6)[40] in reasonably short times (3-15 hours). Initially, negligible differences were observed in aliquots analyzed after 3 and 15 hours of reaction time (M_n = 10.0 kDa, ĐM = 1.59 after 3h and M_n = 10.6 kDa, ĐM = 1.64 after 15 h). Other polar aprotic solvents such as NMP and HMPA were also tested and the results compared with those from DMAc. These results are summarized in Table 3.1, where it is clear that both solvents have a good influence on the resulting M_n values.

Table 3.1: Influence of solvent on the preparation of ECP-Magenta via DHAP.

Solvent	DC	Time (h)	Yield (%)	M_n (kDa)	$Đ_M$
DMAc	38	15	87	10.0	1.64
NMP	32	24	82	23.0	1.74
HMPA	31	24	80	26.3	2.52

DC = Dielectric constant

Next, we decided to evaluate the evolution of molecular weights, and monomer consumption of the DHAP with time. Small aliquots (~ 1-2 mL) of the reaction mixture were precipitated in a 1:1 conc. HCl/MeOH mixture, extracted with DCM, and concentrated. The resulting polymers were analyzed by GPC and 1H-NMR. The plot of M_n and ĐM versus polymerization time of each aliquot can be seen in Figure 3.1 below.

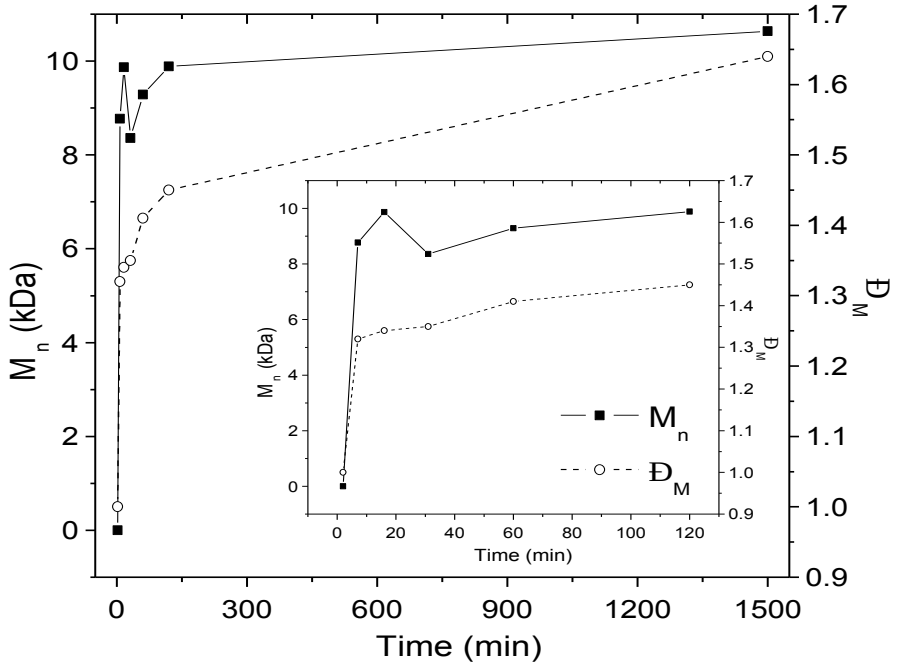

Figure 3.1: Plot of Mn (filled rectangles) and ĐM (open circles) values versus time for the synthesis of ECP-Magenta via DHAP in DMAc.

This data suggests that the polymer chains grow to a size that tends to remain constant with polymerization time which, coupled with the relatively small ĐM values, a chain-growth polymerization mechanism could be initially considered.[41] However, the GPC traces shown in Figure 3.2 highlight polymer formation is observed at short time scales (~2 min) as well as the formation of shorter chains, which disappear from the mixture after 24 h.

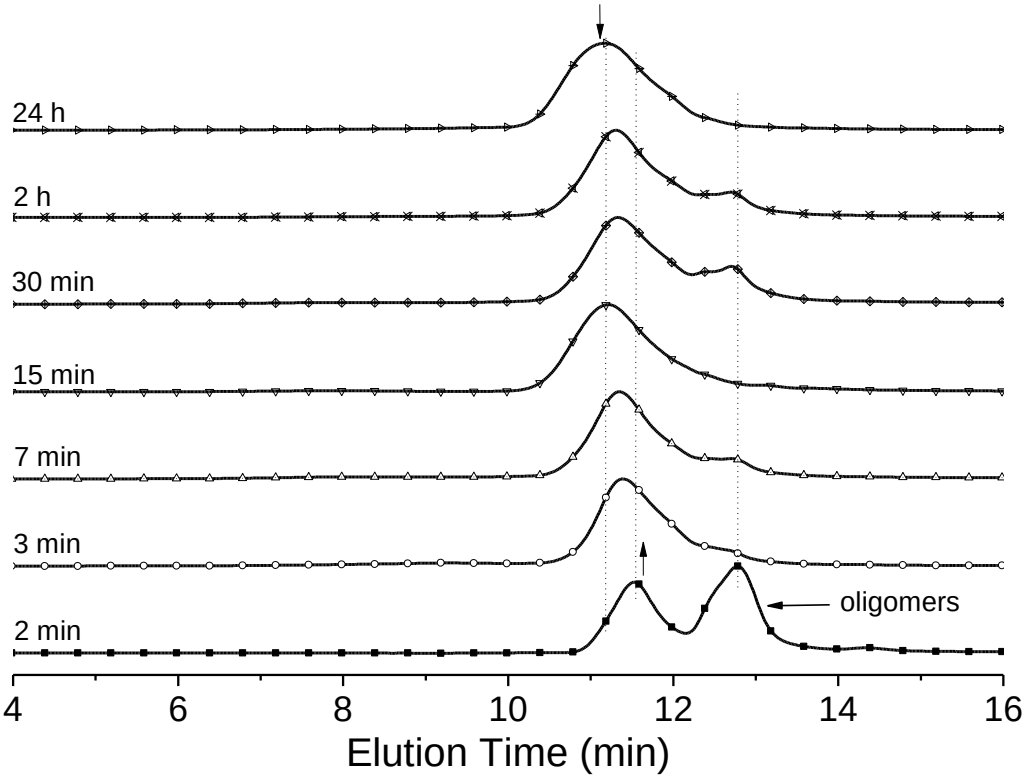

Figure 3.2: Evolution of the GPC traces for the DHAP reaction for the generation of ECP-Magenta.

The previous results presented above prompted us to take a closer look at the evolution of monomer concentration in solution, thus the polymerization was carried out again in the presence of dodecane as an internal standard. Aliquots from the polymerization mixture were subjected to GC-MS and the results, shown in Figure 3.3, clearly show that the starting monomers are consumed within 2-3 minutes.

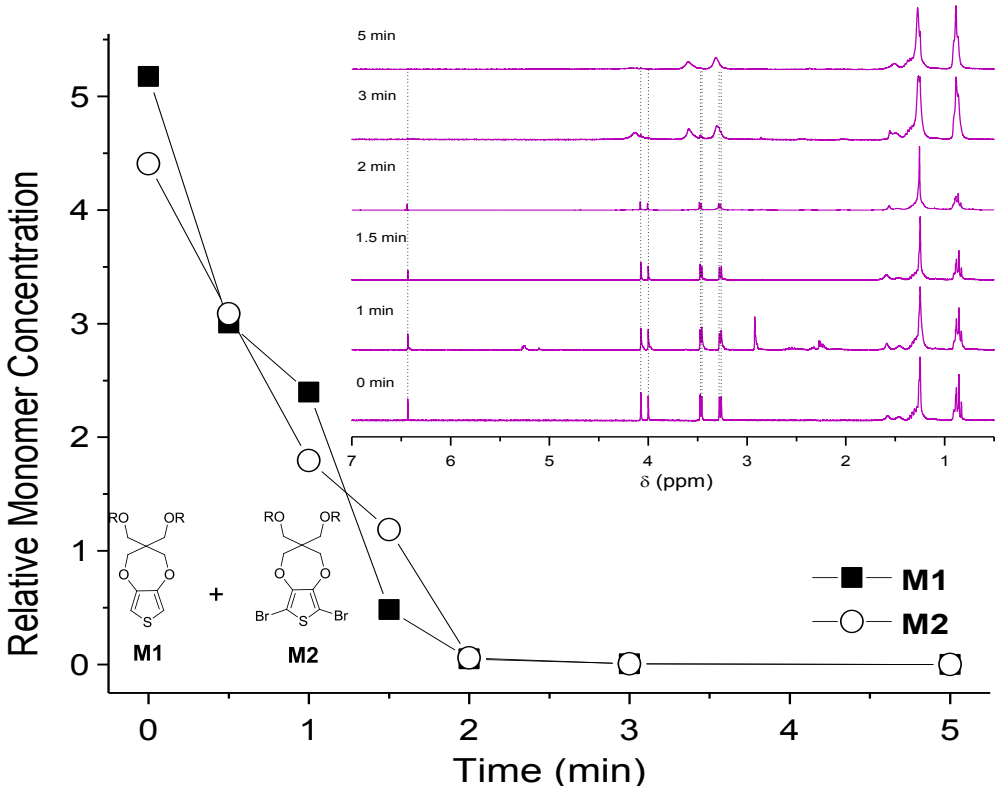

Figure 3.3: Plot of relative concentration of monomers M1 and M2 with respect to dodecane (internal standard) as judged by GC-MS. Inset: ^{1}H NMR signal evolution of the different aliquots taken from this polymerization.

This information correlates well to the ^{1}H NMRs of the aliquots taken from solutions without dodecane, which are shown in the inset for comparison. (For comparison, Figure 3.4 offers the ^{1}H NMR traces of the individual components).

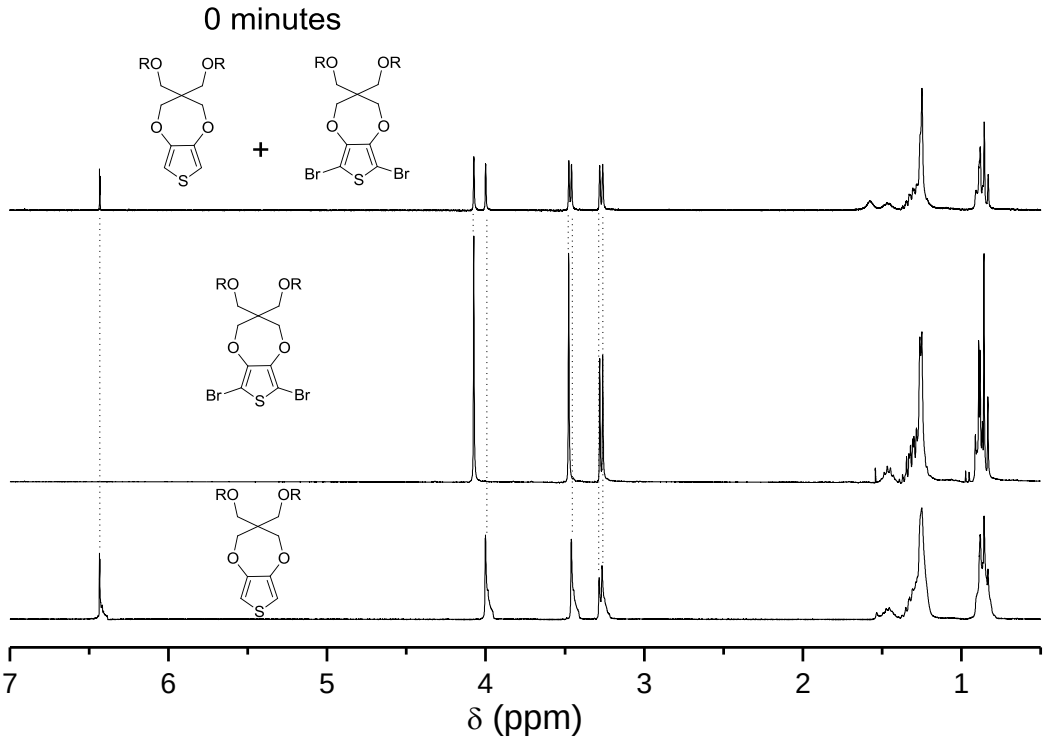

Figure 3.4: Spectral comparison of the ^{1}H NMR signals of compounds (**1**) and (**2**) individually and as mixture.

Thus, it is clear the monomers are totally consumed prior to the weight evolution of the polymer and that the relationship between monomer conversion and M_n of the polymer is nonlinear.

The DHAP of the monobrominated adduct (**M3**), instead of the nonbrominated (**M1**)/dibrominated (**M2**) mixture, was also evaluated (case B). Figure 3.5 shows a similar behavior for the consumption of the starting materials for both cases at t < 3 min, where it is evident that the **M1**/**M2** reaction (case A) proceeds faster.

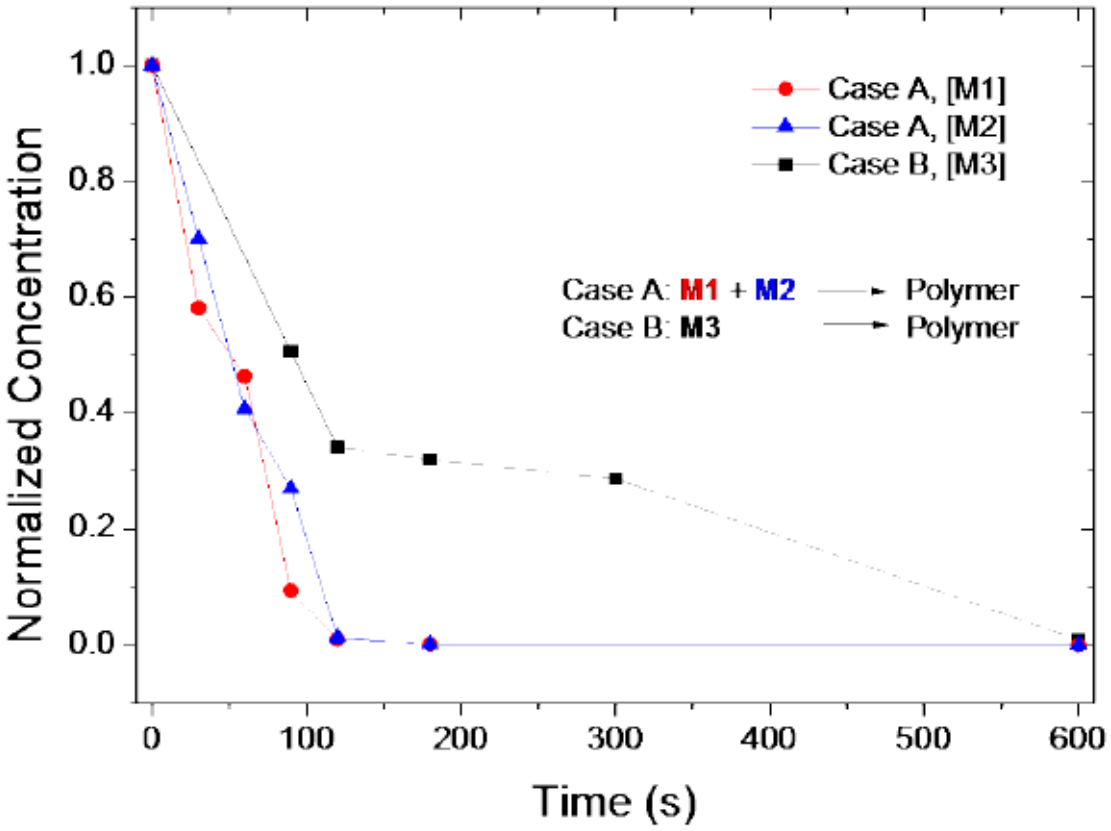

Figure 3.5: Plot of [X] vs. time under DHAP conditions where X = **M1**/**M2** for case A, and **M3** for case B. For case A, the consumption of the starting materials is faster than for case B.

Additionally, the reaction kinetics of the DHAP of **M3** is analogous to that reported by Ozawa et al. on the DHAP of 2-bromo-3- hexylthiophene (2B3HT) using Pd(otolyl) 3 and a phosphine cocatalyst.[41] We have found that our conditions render a faster reaction, however: the stage obeying first-order kinetics with respect to the concentration of **M3** presents in our case a $k_{obs} = (8 \pm 1) \times 10^{-3}$ s^{-1}, which is two orders of magnitude larger than that observed for Ozawa for the synthesis of P3HT from 2B3HT.[41]

The polymer, freshly prepared as mentioned above, was then subjected to a more thorough cleansing procedure: it was redissolved in chlorobenzene at 50 °C and treated with a Pd-scavenger (diethylammonium diethyldithiocarbamate) and 18-crown-6 to remove the residual Pd and K metals (see details in section 3.5 Polymerization

Procedures). After the polymer was precipitated in MeOH, it was filtered and washed with MeOH, then hexanes. Finally, the polymer was dried under vacuum overnight. This rigorous purification procedure showed little differences in the M_n values (+2-3%) signifying losses of only lower molecular weight material as expected. Furthermore, no observable differences were detected in the ^{1}H NMR spectra (Figure 3.6).

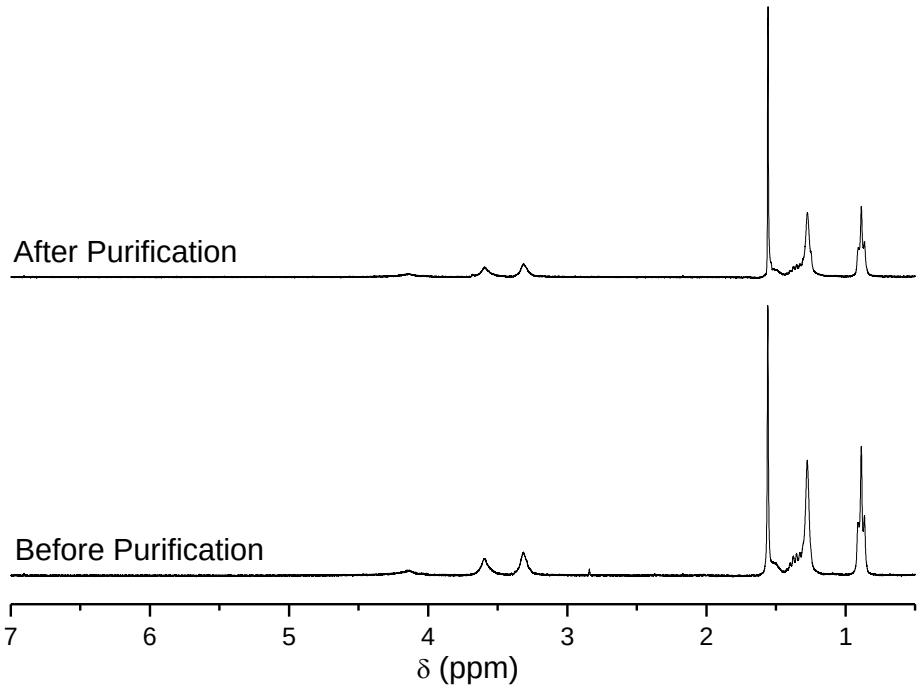

Figure 3.6: Spectral comparison of the ^{1}H NMR signals of ECP-Magenta before and after purification.

The residual content of representative elements was determined by ICP-MS from polymer samples subjected to similar purifications procedures but created from different polymerization methods. This is illustrated in Figure 3.7 where it is clearly shown that the metal content displayed by the polymers made via DHAP is less than 20 ppm for all cases.

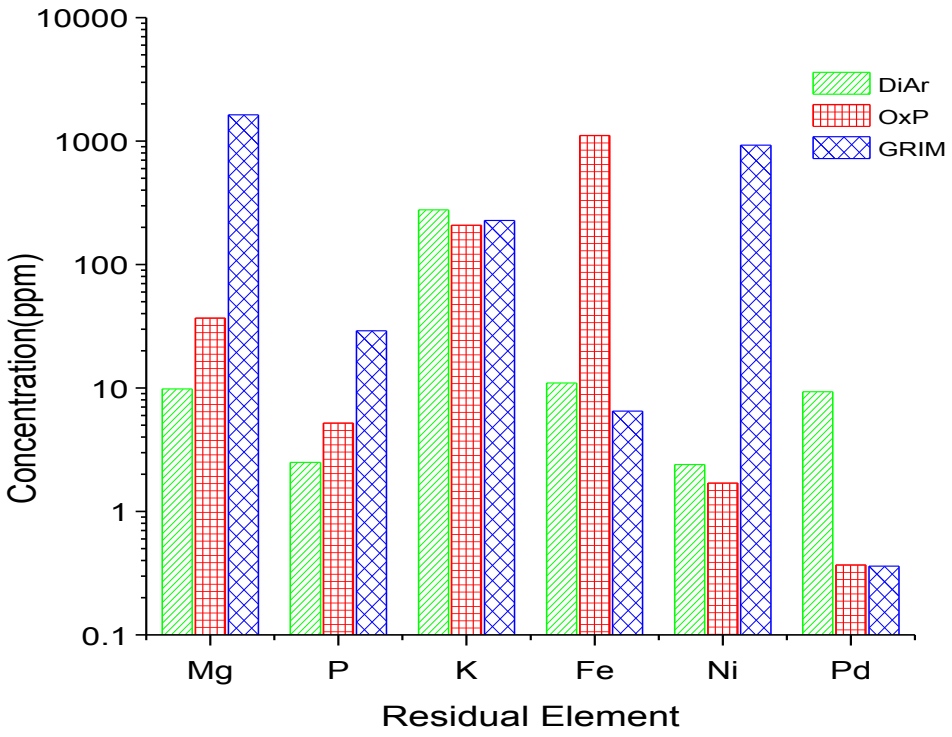

Figure 3.7: Residual content of selected elements for polymers obtained via DHAP, OxP, and GRIM.

For example, the OxP utilizes more than 4 equivalents of $FeCl_3$ which results in a high content of elemental Fe (> 1,000 ppm). All other selected elements were low in content. GRIM polymerization displayed great contents of Mg and Ni (> 900 ppm) as judged by the use of these metals in the polymerization. While the presence of phosphorous is relatively larger than the other two polymerization procedures, these are not significantly large (less than one order of magnitude). While the potassium content is an important consideration, technical limitations of our ICP instrument hampered its study. The relative values were unresolved due to the large K background signal. Figure 3.8 provides the residual content for selected elements, as measured by ICP-MS from ECP-Magenta samples synthesized in DMAc, NMP, and HMPA before and after purification. Interestingly, the sample synthesized from HMPA displayed the highest content of Pd before and after purification (~30−50 times those of DMAc/NMP samples). The higher

number of residual phosphorus implies the presence of HMPA in the polymer (i.e., it is the only source of phosphorus), which makes us consider that HMPA could be binding Pd.

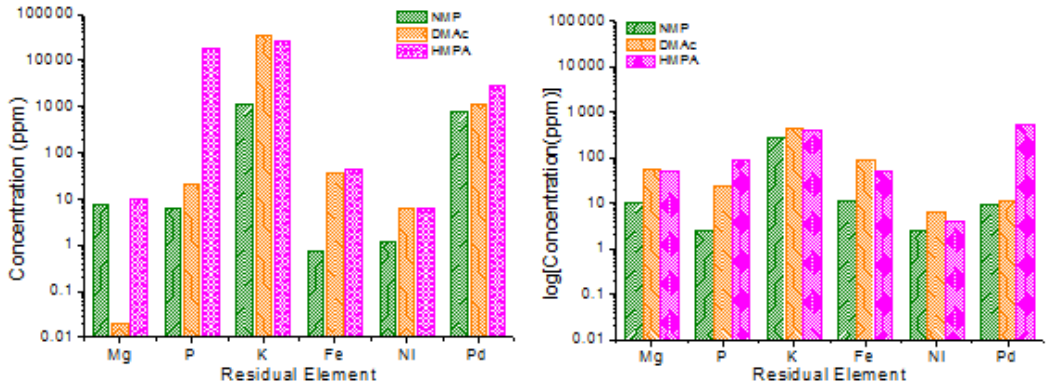

Figure 3.8: Residual content of selected elements for polymers obtained via DHAP from different solvents though the ICP-MS technique. (**A**) Before purification. (**B**) After purification.

Figure 3.9 provides the UV−vis absorption and emission spectra of the toluene solutions of polymers synthesized by different methods. Their absorption was identical, except in the low energy maximum localized at 595 nm, which is more intense in the case of the GRIM and DHAP generated polymers (DMAc).

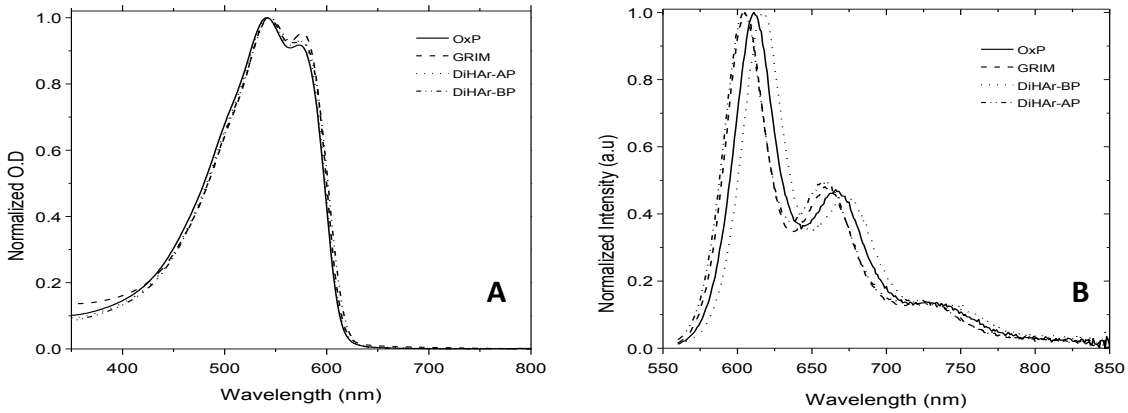

Figure 3.9: Steady state UV-Vis spectra of polymer samples (**A**) Absorption. (**B**) Fluorescence

These solutions follow Lambert−Beer law at the 1−10 mg/mL concentration regime, shown in Figure 3.10 below:

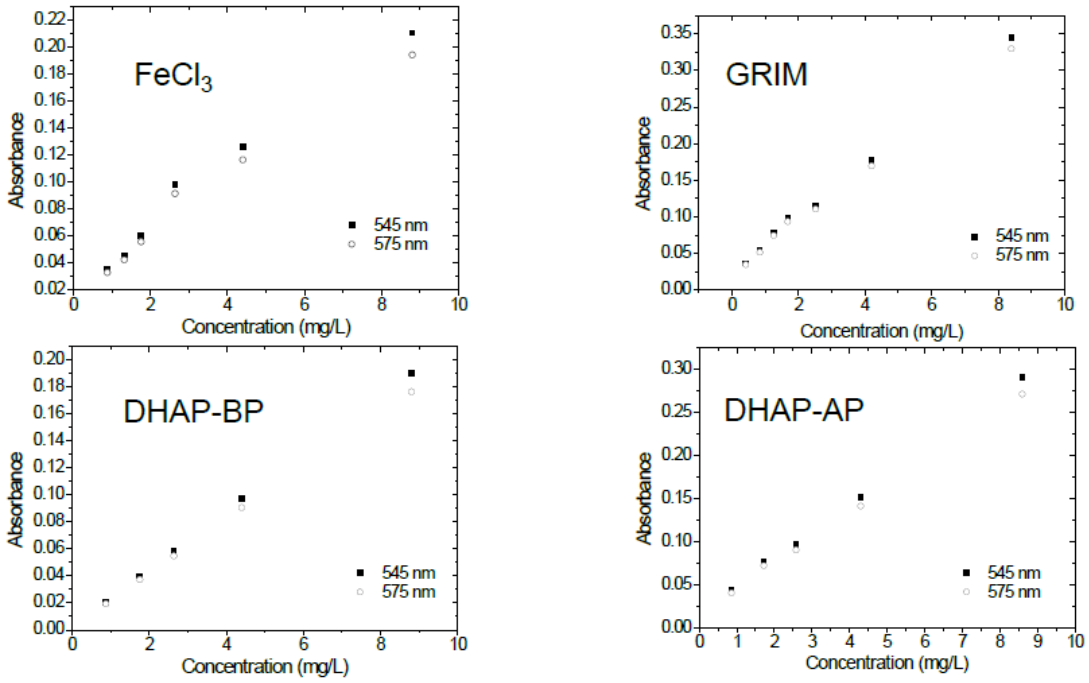

Figure 3.10: Plot of mass concentration vs. Absorbances for ECP-Magenta Samples synthesized though various synthetic methods (DHAP is presented before and after purification). Probe wavelengths: 454 and 575 nm.

However, the solution fluorescence differs more noticeably; the OxP and DHAP polymer before purification presented the reddest shifted spectra and the other two polymers, GRIM and DHAP after purification, presented almost identical spectra. Figure 3.11 illustrates that samples with O.D. ≤ 0.1 show linear behavior in their fluorescence intensity.

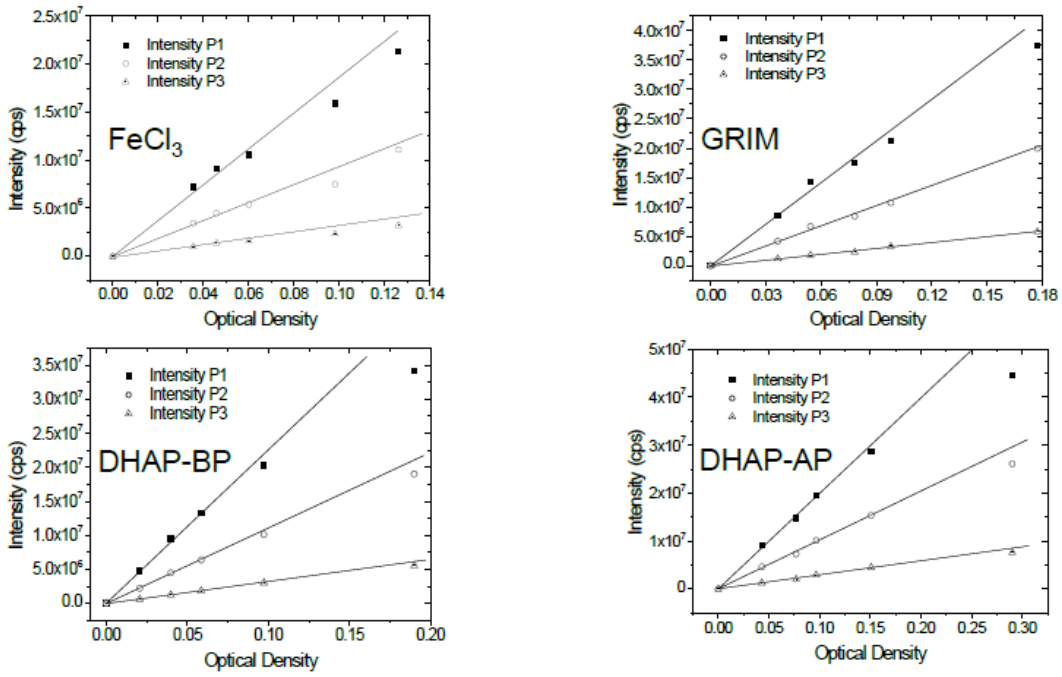

Figure 3.11: Plots of Optical Densities vs. Fluorescence Intensities for ECP-Magenta Samples (probe wavelengths: 605-610 (P1), 660-666 (P2), and 725-734 (P3) nm bands)

Also, the fluorescence gradients from these polymers presented in Figure 3.12 are comparable. The lower fluorescence yield of the DHAP sample before purification illustrates the effect of residual Pd content in promoting nonradiative decay paths, presumably via intersystem crossing through external heavy atom effect.[43] Technical restrictions precluded the acquisition of the emission lifetimes, as these are shorter than the pulses of our nano LED source (~1.2−1.4 ns).

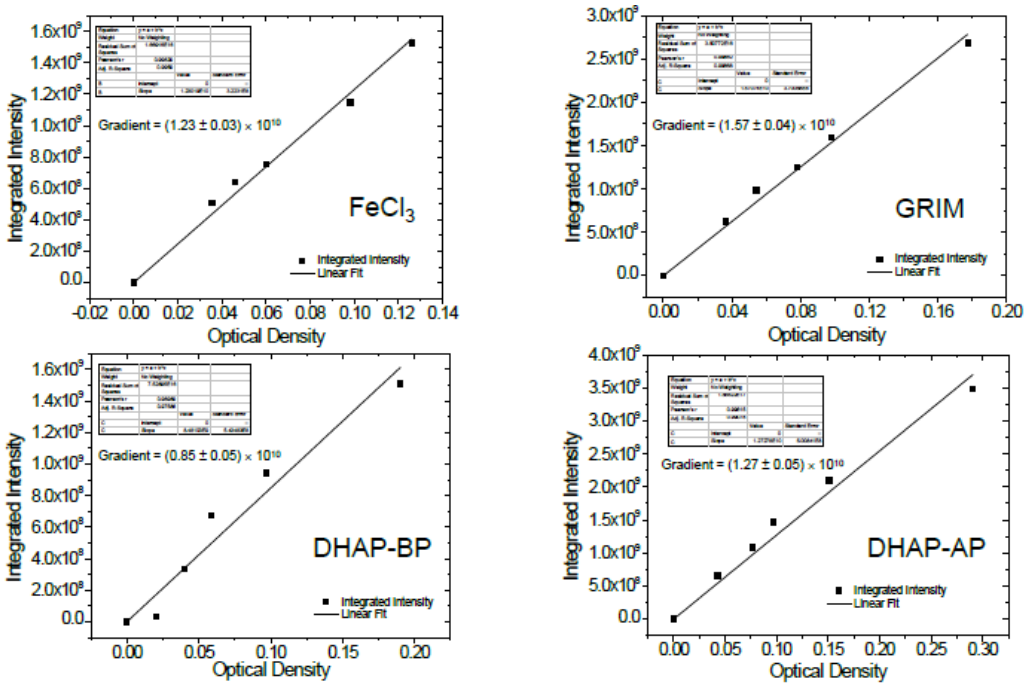

Figure 3.12: Plots of Fluorescence Gradients for ECP-Magenta

Given the promising results obtained up to this stage, we decided to test the flexibility of the DHAP conditions for the preparation of alternating copolymers. As an initial example, copolymerization of 4,7-dibromo-2,1,3-benzothiadiazole with monomer M1 in NMP afforded ECP-blue[44] in high yields with M_n = 9.4 kDa and ĐM = 1.54. From this success, we expanded this protocol to complete the full CMYK palette: cyan, [45] yellow, [46] and black.[47] The structures of all synthesized polymers are shown in section Figure 3.13. All attempts afforded us with polymers of high molecular weight in good yields, comparable to those previously reported except for ECP-blue.[42–45] The pertinent characterization data for all polymers are summarized in Table 3.2 below:

Table 3.2: Scope of DHAP for the synthesis of ECPs.

Polymer	Yield (%)	M_n (kDa)	$Đ_M$	DP
ECP-Magenta	82	23.0	1.74	52
ECP-Yellow	76	27,5	1.19	53
ECP-Blue	81	9,41	1.54	16
ECP-Cyan[a]	89	---	---	--
ECP-Black	76	11.0	2.03	--

a. This polymer was not soluble in THF at the required concentrations for successful GCP analysis.

In the case of ECP-cyan, the ^{1}H NMR data are identical to those of the reported sample synthesized via OxP.24 We believe that the DHAP sample presents higher M_n values than the reported polymer since its insolubility in THF prevented the GPC characterization. Toluene solutions of these polymers were sprayed on ITO slides and characterized by means of UV−vis spectrophotometry.

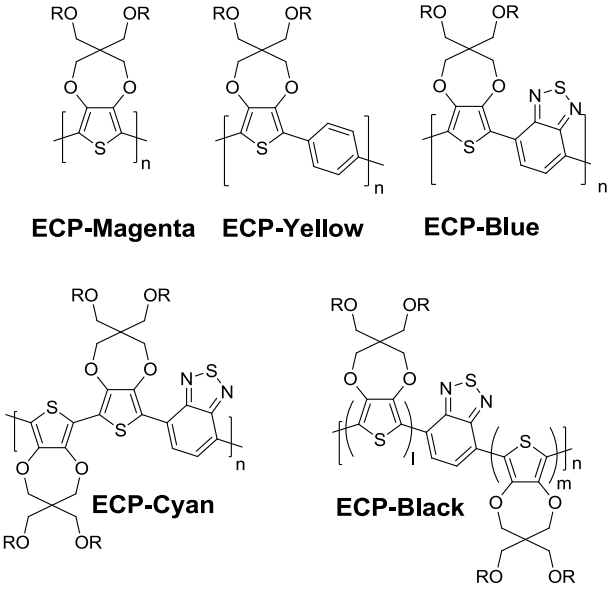

Figure 3.13: Synthesized ECP polymers

As shown in Figure 3.14, the ECP-magenta film exhibits good color purity and excellent contrast (Δ%T = 79% at 530 nm) comparable to the best performing polymers previously reported (Δ%T = 80% at 609 nm).[36] Interestingly, the contrast is steady in spite of the lower amounts of residual metal content from the DHAP samples.

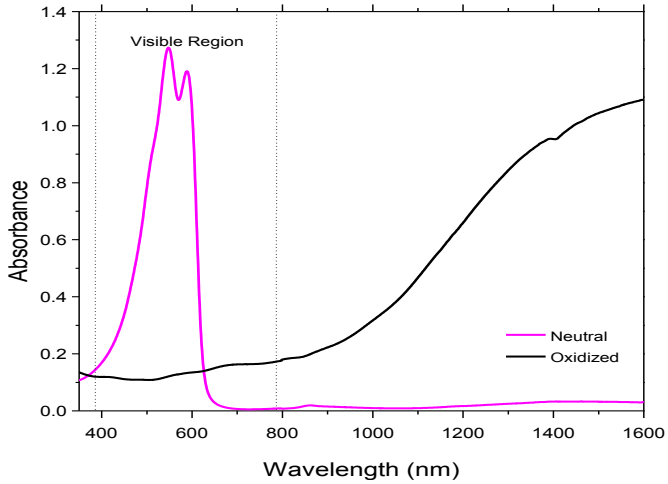

Figure 3.14: UV-Vis spectra of ECP-Magenta in neutral and oxidized forms (V = +0.8 V vs $Ag|Ag^{+}$).

By comparing the spectroelectrochemical curves of these polymers with those reported in the literature,[42-45] we see no remarkable differences in performance from polymers that were synthesized through other Pd-catalyzed cross-coupling reactions (Figures 3.15 and 3.16), except for the case of ECP-blue, whose contrast was smaller than that reported by us for a polymer with higher M_n.[44]

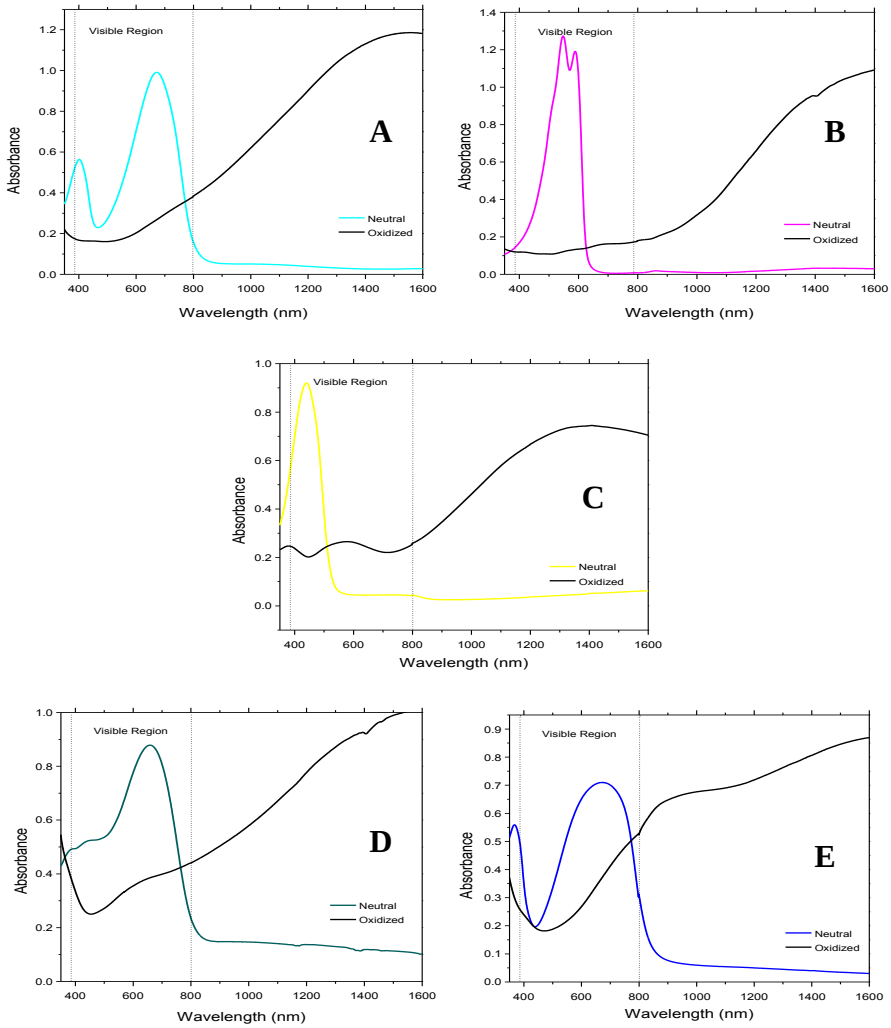

Figure 3.15. UV-Vis-NIR spectra of the neutral (colored line) and oxidized (black line) species of ECPs obtained via DHAP. Applied potentials vs. $Ag|Ag^{+}$ were (**A**) ECP-Cyan: −0.10 and 0.90 V, (**B**) ECP-Magenta: −0.10 and 0.80 V, (**C**) ECP-Yellow: 0.00 and 1.00 V, (**D**) ECP-Black: 0.00 and 0.65 V (**E**) ECP-Blue: 0.00 and 0.90 V.

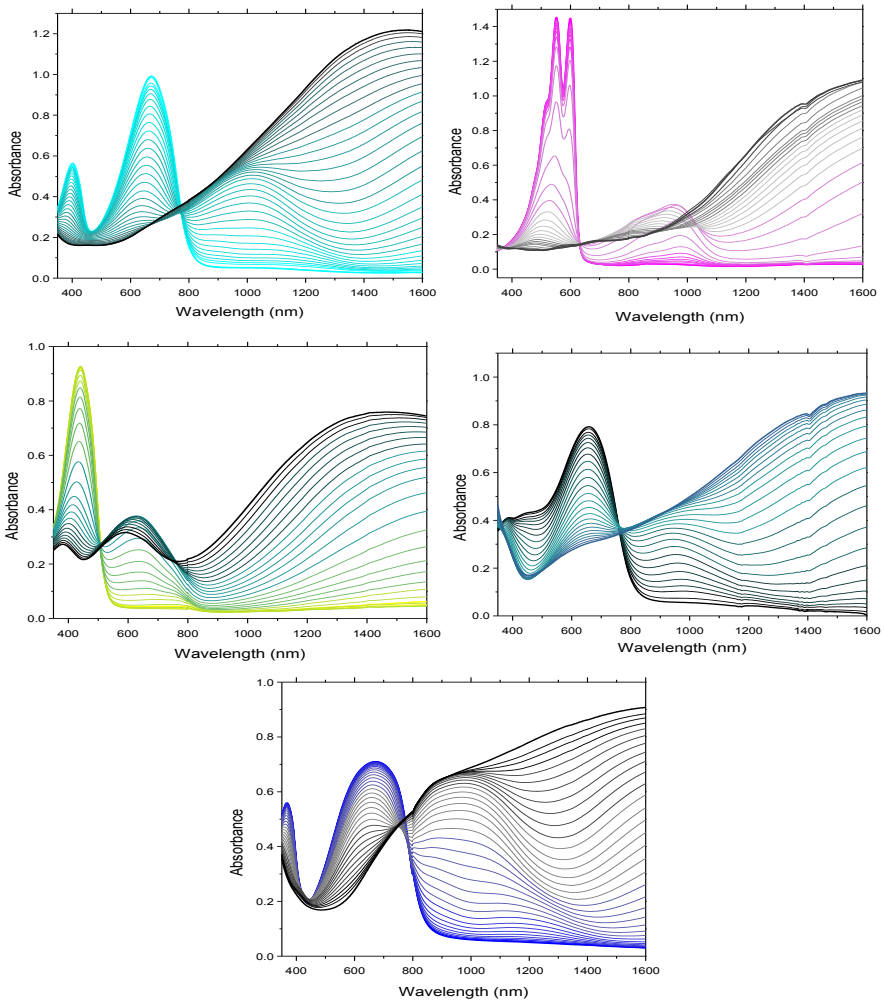

Figure 3.16: Spectral evolution for the UV-Vis-NIR absorption of ECPs obtained via DHAP with respect to potential steps of 25 mV. Applied potentials vs. $Ag|Ag^{+}$ were in the range of: (**A**) ECP-Cyan (−0.10,0.90) V, (**B**) ECP-Magenta (−0.10,0.80) V, (**C**) ECP-Yellow (0.00,1.00) V, (**D**) ECP-Black (0.00,0.65) V (**E**) ECP-Blue (0.00,0.90) V.

This implies that the contrast is a function that could be more dependent on the M_n of the polymer rather than the residual impurities. Given the atom economy, shorter times, and simpler purification procedures, we envision the DHAP methodology to reduce costs for the synthesis of ECPs that render the full color palette.

3.3 Materials and Equipment Utilized

Commercially available reagents were used as received from the chemical suppliers. Reactions that required anhydrous conditions were carried out under an inert atmosphere of argon in flame-dried glassware. Toluene and THF were dried using a solvent purification system (MBraun MB Auto-SPS). The rest of solvents used for synthetic purposes were purified using conventional protocols,[i] except glacial acetic acid which was used as received. All reactions were monitored using F250 silica gel 60 M analytical TLC plates, with UV detection (λ = 254 and 365 nm). Silica gel (60Å, 40–63 μm) was used as stationary phase for column chromatography. NMR experiments were acquired with working frequencies of 300 MHz for ^{1}H, and 75.5 MHz for ^{13}C experiments. The shifts were reported in parts per million (ppm) and referenced to the residual resonance signals of commercially available deuterated chloroform: δ_H=7.26 ppm, δ_C=77.0 ppm.[ii] High-resolution mass spectra were recorded on a quadrupole mass analyzer instrument equipped with a direct insertion probe (ionization 70 eV) and an electron spray ionizer. Gel permeation chromatography (GPC) was performed using a Waters Associates GPCV2000 liquid chromatography with is internal differential refractive index detector at 40 °C, using two Waters Styragel HR-5E column (10 mm PD, 7.8 mm i.d., 300 mm length) with HPLC grade THF as the mobile phase at flow rate of 1.0 mL/min. The polymer was dissolved initially in THF (2 mg/mL), and allowed to solubilize for 24-48 hour period, in which the solution was filtered through a Millipore 0.5 μm filter. Injections of ~200 μL were performed and retention times were calibrated against narrow molecular weight polystyrene standards.

All reagents used for ICP-MS elemental analyses were Optima-grade and the sample preparation was done under a clean lab environment in the Department of Geological Sciences at the University of Florida. Polymer samples were digested in pre-cleaned Savillex PFA vials (http://www.savillex.com) with aqua regia (3 mL HCl and 1 mL HNO_3) overnight on a hot plate at 120°C. During the aqua regia digestion the polymer samples turn into a yellowish transparent mass. Although not complete dissolution of the polymer is achieved, it is expected that the elements of interest will be transferred quantitatively in solution. After digestion, part of the aqua regia solution is further diluted with 5% HNO_3 and loaded in the ICP-MS for analysis. Elemental analyses were

performed on a ThermoFinnigan Element2 HR-ICP-MS in medium resolution mode. Quantification of results was done by external calibration using a combination of commercially available standards (http://www.exaxol.com and http://www.qcdanalysts.com) gravimetrically diluted to appropriate concentrations. All concentrations are reported in ppm in the polymer.

Electrochemistry was carried out in 0.1 M $TBAPF_6$/propylene carbonate solutions, using a standard 3-electrode system: the reference electrode was $Ag|Ag^+$ (10 mM $AgNO_3$/0.5 M $TBAPF_6$/ACN solution) calibrated against the $Fc|Fc^+$ ($V_{Fc/Fc+}$ = 81 mV), the counter electrode was a Pt-wire, and the working electrode was an ITO-coated glass slide (7×50×0.7 mm^3, 20 Ω/sq) from Delta Technologies Ltd. Propylene carbonate was dried using a Vacuum Atmospheres SPS. All electrochemical measurements were carried out using an EG&G PAR galvanostat/potentiostat PC-controlled using Scribner Associates 169 CorrWare II software. Absorption spectra were recorded in a double-beam Varian Cary 5000 UV-Vis-NIR spectrophotometer; the baseline correction included solution, ITO-slide, and glass cuvette. Fluorescence spectra were recorded in a Fluorolog-1057 from Horiba-Jovin-Yvon: the samples were excited using a standard 450 W xenon CW lamp and the fluorescence was detected using a multialkali PMT (250-850 nm). Correction factors for lamp signal and detector dark counts were applied using the FluorEssence® software from HJY.

3.4 Synthetic Procedures and Characterization of Monomers

6,8-dibromo-3,3-bis((2-ethylhexyloxy)methyl)-3,4-dihydro-2H-thieno[3,4-b][1,4]dioxepine (2) and 6-bromo-3,3-bis((2-ethylhexyloxy)methyl)-3,4-dihydro-2H-thieno[3,4-b][1,4]dioxepine (3): 3,3-bis((2-ethylhexyloxy) methyl)-3,4-dihydro-2H-thieno[3,4-b][1,4]dioxepine (**1**, 12.1 g, 27.5 mmol) was dissolved in chloroform (50 mL) and covered from light using aluminum foil. After cooling the mixture in an ice/water bath, N-bromosuccinimide (5.4 g, 30.2 mmol) was added in small portions. The bath was removed, and the mixture was allowed to react for 8 hours at room temperature. Water (25 mL) was added at once and the heterogeneous mixture was transferred to a separation funnel. After shaking, the layers were separated and the aqueous mixture was further

extracted with DCM (3×50 mL). The organic mixtures were combined, dried over $MgSO_4$, filtered and evaporated to dryness. The residual light yellow oil was purified via column chromatography in hexanes where the monobrominated and dibrominated product.

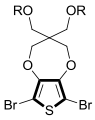

2

6,8-dibromo-3,3-bis((2-ethylhexyloxy)methyl)-3,4-dihydro-2H-thieno[3,4-b][1,4]dioxepine (**1**): Light yellow oil. 6.4 g, 39% yield. This compound has been reported previously.[iii] Characterization data agreed accordingly (MS, ^{1}H NMR) ^{1}H NMR (300 MHz, $CDCl_3$, δ): 4.09 (s, 4H), 3.47 (s, 4H), 3.24 (d, 4H), 1.2-1.6 (m,18H), 0.8-1.0 (m, 12H). LRMS: [$M^{\bullet+}$] 598.51, expected for $C_{25}H_{42}O_4SBr_2$: 598.47.

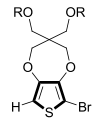

3

6,8-dibromo-3,3-bis((2-ethylhexyloxy)methyl)-3,4-dihydro-2H-thieno[3,4-b][1,4]dioxepine (**3**): Light yellow oil. 4.7 g, 33% yield. ^{1}H NMR (300 MHz, $CDCl_3$, δ):6.44 (s, 1H), 3.98-4.10 (d, *J* = 2.4 Hz, 4H), 3.47 (s, 4H), 3.24-3.30 (d, *J* = 0.6 Hz, 4H), 1.15-1.55 (m, 18H), 0.80-0.95 (m, 12H). HRMS: [$M^{\bullet+}$] 518.2052, expected for $C_{25}H_{43}O_4SBr$: 518.2065.

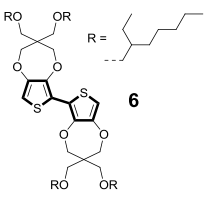

6

3,3,3',3'-tetrakis(((2-ethylhexyl)oxy)methyl)-3,3',4,4'-tetrahydro-2H,2'H-6,6'-bithieno[3,4 -b][1,4]dioxepine (6): 3,3-bis((2-ethylhexyloxy) methyl)-3,4-dihydro-2H-thieno[3,4-b] [1,4]dioxepine (**1**, 2.0 g, 4.5 mmol) was dissolved in anhydrous THF (25 mL) under argon. The mixture was cooled in a dry ice/acetone bath followed by dropwise addition of n-BuLi (2.89 M in hexanes, 1.6 mL, 0.5 mmol). The yellow mixture was warmed up in an ice/water bath and once equilibrated, it was slowly transferred to a suspension of $Fe(acac)_3$ in THF at room temperature via cannula. The mixture was heated to gentle reflux temperature and allowed to stir overnight. The resulting suspension was filtered through a pad of silica gel and eluted with hexanes until no product was found in the filtrate (monitored by TLC). The resulting organic solution was evaporated to dryness and purified via flash chromatography using hexanes as eluant. Colorless oil was obtained (1.35 g, 68 % yield). ^{1}H NMR (300 MHz, $CDCl_3$, δ):6.36 (s, 2H), 4.00-4.12 (d, *J* = 2.4 Hz, 8H), 3.50 (s, 8H), 3.25-3.31 (d, *J* = 0.6 Hz), 1.42-1.54 (m, 4H), 1.20-1.42 (m, 36H), 0.80-1.00 (m, 24H). HRMS: [$M^{\bullet+}$] 878.5743, expected for $C_{50}H_{86}O_8S_2$: 878.5764.

3.5 Polymerization Procedures

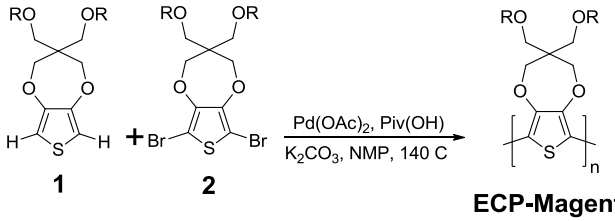

ECP-Magenta (A): To a oven dried Schlenk tube fitted with a magnetic stir bar $Pd(OAc)_2$ (2.25 mg, 2 mol%), K_2CO_3 (173 mg, 1.3 mmol), and Pivalic Acid (0.01 g, 0.15 mmol) were added sequentially. The reaction flask was evacuated for a total of ten minutes, and purged with anhydrous argon. This evacuation/gas filling procedure was repeated three times. A separate vial was loaded with 6,8-dibromo-3,3-bis((2-ethylhexyloxy)methyl)-3,4-dihydro-2H-thieno[3,4-b][1,4]dioxepine (**1**, 299 mg, 0.5 mmol), and 3,3-bis((2-ethylhexyloxy)methyl)-3,4-dihydro-2H-thieno[3,4-b][1,4]dioxepine (**2**, 220mg, 0.5 mmol). After evacuating for 10 minutes, argon saturated NMP (2 mL) was added via argon flushed syringe. The resulting solution was transferred to the mother Schlenk tube via syringe in one portion. The vial was then washed twice with 2 mL of Ar-saturated DMAc where each washing was transferred to the reaction flask. Afterward, the combined reagents were put into a 140 °C oil bath and allowed to stir for three hours. Upon cooling to room temperature, the mixture was poured into 50 mL of a 1:1 MeOH/1M HCl aqueous solution with vigorous stirring. The resulting precipitate was filtered, washed with water (5 × 10 mL), then MeOH (3×10 mL), and finally suction dried for 15 minutes. The resulting solid was suspended in 50 mL of chlorobenzene and heated to 60 °C. Once the solids dissolved completely, diethyl dithiocarbamic acid diethylammonium salt (Pd-scavenger, 2.0 mg, ~ 4 eq of Pd content) and 18-crown-6 (1.3 g, 5 mmol) were added and the solution was stirred for 4 hours. The reaction mixture was cooled to room temperature, and precipitated into MeOH. The precipitate was filtered by gravity filtration, washed with MeOH (5×10 mL), then hexanes (3 × 5 mL) and dried under vacuum overnight. A total of 388 mg of dark maroon powder was obtained (88% yield). This polymer has been previously reported.[iii] Characterization data agreed accordingly. ^{1}H NMR (300 MHz, $CDCl_3$, δ): 4.15 (bs, 4H),

3.60 (bs, 4H), 3.33 (bs, 4H), 1.52 (bs, 4H), 1.20-1.45 (m, 18H), 0.82-0.94 (m, 12H). GPC (THF, PS): M_n = 9,980 g/mol, Đ = 1.42.

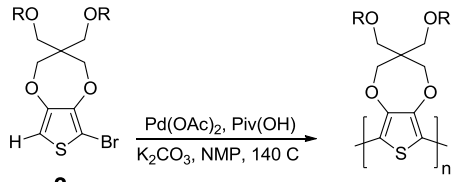

3 **ECP-Magenta**

ECP-Magenta (B): This material was prepared following exactly the procedure described for ECP-Magenta with the following modifications: all solid materials were loaded into the oven dried Schlenk. In a separate vial, 6-bromo-3,3-bis((2-ethylhexyloxy)methyl)-3,4-dihydro-2H-thieno[3,4-b][1,4]dioxepine (**3**, 299 mg, 0.5 mmol) was weighed. The sequences of evacuation/purging, plus reactant mixing is exactly the same as the general procedure. Once all reactants were mixed altogether, the tube was inserted into the oil bath preheated at 140 °C. After 3 hours, the resulting yellow mixture was worked up and the resulting polymer was isolated as previously described for ECP-Magenta. A total of 210 mg of dark purple-colored powder was obtained (95% yield). All characterization data matched the ones previously described for ECP-Magenta. GPC (THF, PS): M_n = 9,440 g/mol, Đ = 1.42.

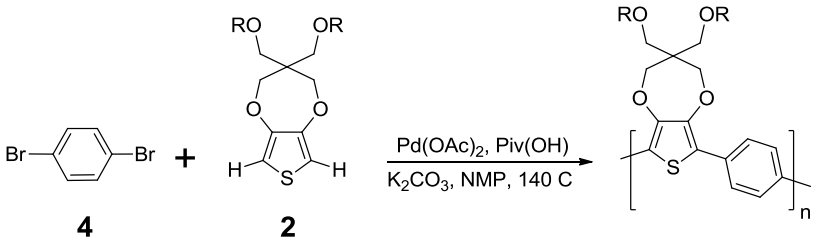

4 **2** **ECP-Yellow**

ECP-Yellow: This material was prepared following exactly the procedure described for ECP-Magenta with the following modifications: all solid materials were loaded into the oven dried Schlenk tube including this time 1,4-dibromobenzene (**3**, 118 mg, 0.5 mmol). In a separate vial, 3,3-bis((2-ethylhexyloxy)methyl)-3,4-dihydro-2H-thieno[3,4-b][1,4]dioxepine (**2**, 220 mg, 0.5 mmol) was weighed. The sequences of evacuation/purging, plus reactant mixing is exactly the same as the general procedure. Once all reactants were mixed altogether, the tube was inserted into the oil bath preheated at 140 °C. After 3 hours, the resulting yellow mixture was worked up and the resulting

polymer was isolated as previously described for ECP-Magenta. A total of 210 mg of dark orange-colored powder was obtained (76% yield). This polymer has been previously reported.[iv] Characterization data agreed accordingly. ^{1}H NMR (300 MHz, $CDCl_3$, δ): 7.75 (bs, 4H), 4.19 (bs, 4H), 3.60 (bs, 4H), 1.52 (bs, 4H), 1.22-1.44 (m, 18H), 0.82-0.98 (m, 12H). GPC (THF, PS): M_n = 27,500 g/mol, Đ = 1.19.

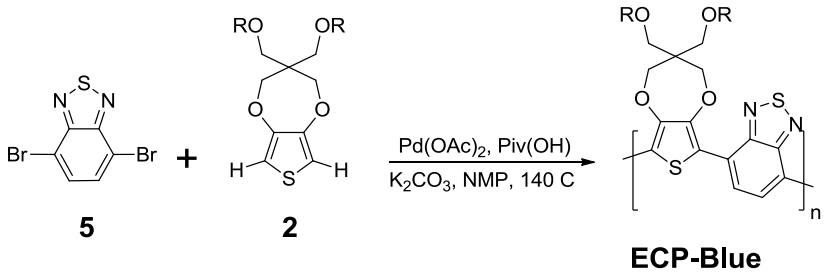

5 **2** **ECP-Blue**

ECP-Blue: This material was prepared following exactly the procedure described for ECP-Magenta with the following modifications: all solid materials were loaded into the oven dried Schlenk tube including this time 4,7-dibromo-2,1,3-benzothiadiazole (**4**, 147 mg, 0.5 mmol). In a separate vial, 3,3-bis((2-ethylhexyloxy)methyl)-3,4-dihydro-2H-thieno[3,4-b][1,4]dioxepine (**2**, 220 mg, 0.5 mmol) was weighed. The sequences of evacuation/purging, plus reactant mixing is exactly the same as the general procedure. Once all reactants were mixed altogether, the tube was inserted into the oil bath preheated at 140 °C. After 3 hours, the resulting dark blue mixture was worked up and the resulting polymer was isolated as previously described for ECP-Magenta. A total of 375 mg of dark blue-colored (almost black) powder was obtained (81% yield). This polymer has been previously reported.[v] Characterization data agreed accordingly. ^{1}H NMR (300 MHz, $CDCl_3$, δ): 8.42 (bs, 2H), 4.33 (bs, 4H), 3.65 (bs, 4H), 3.35 (bs, 4H), 1.20-1.60 (m, 22H), 0.85-0.98 (m, 12H). GPC (THF, PS): M_n = 9,440 g/mol, Đ = 1.54.

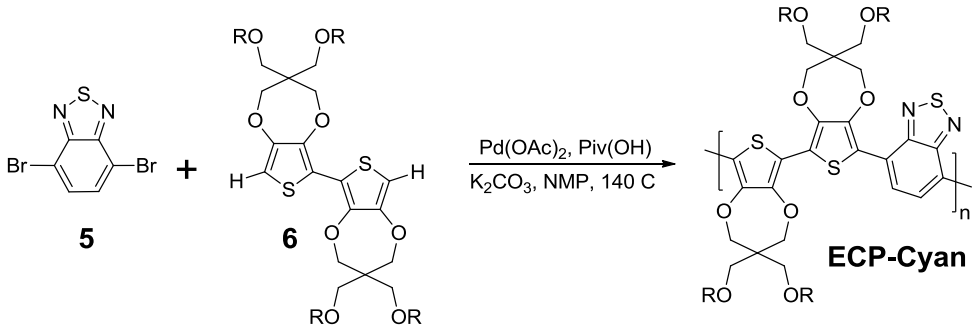

5 **6** **ECP-Cyan**

ECP-Cyan: This material was prepared following exactly the procedure described for ECP-Magenta with the following modifications: all solid materials were loaded into the oven dried Schlenk tube including this time 4,7-dibromo-2,1,3-benzothiadiazole (**4**, 147 mg, 0.5 mmol). In a separate vial, 3,3,3',3'-tetrakis(2-ethylhexyloxymethyl)-3,3',4,4'-tetrahydro-2H,2'H-6,6'-bithieno[3,4-b][1,4]dioxepine (**2**, 440 mg, 0.5 mmol) was weighed. The sequences of evacuation/purging, plus reactant mixing is exactly the same as the general procedure. Once all reactants were mixed altogether, the tube was inserted into the oil bath preheated at 140 °C. After 3 hours, the resulting dark cyan mixture was worked up and the resulting polymer was isolated as previously described for ECP-Magenta. A total of 410 mg of dark blue-colored powder was obtained (89 % yield). This polymer has been previously reported.[vi] Characterization data agreed accordingly. ^{1}H NMR (300 MHz, $CDCl_3$, δ): 8.38 (bs, 2H), 4.26 (bs, 8H), 3.62 (bs, 8H), 3.36 (bs, 8H), 1.16-1.60 (m, 44H), 0.90-0.99 (m, 24H). The sample was sparingly soluble in THF, which precluded its characterization via GPC.

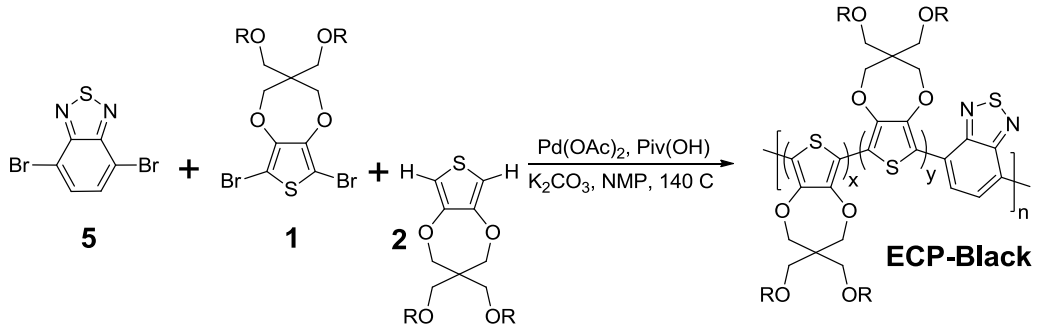

ECP-Black: This material was prepared following exactly the procedure described for ECP-Magenta with the following modifications: all solid materials were loaded into the oven dried Schlenk tube including this time 4,7-dibromo-2,1,3-benzothiadiazole (**4**, 74 mg, 0.25 mmol). In a separate vial, 6,8-dibromo-3,3-bis((2-ethylhexyloxy)methyl)-3,4-dihydro-2H-thieno[3,4-b][1,4]dioxepine (**1**, 150 mg, 0.25 mmol), and 3,3-bis((2-ethylhexyloxy)methyl)-3,4-dihydro-2H-thieno[3,4-b][1,4]dioxepine (**2**, 220 mg, 0.50 mmol) were weighed. The sequences of evacuation/purging, plus reactant mixing is exactly the same as the general procedure. Once all reactants were mixed altogether, the tube was inserted into the oil bath preheated at 140 °C. After 3 hours, the resulting black mixture was worked up and the resulting polymer was isolated as previously described for ECP-Magenta. A total of 395 mg of black-colored powder was obtained (78 % yield).

^{1}H NMR (300 MHz, $CDCl_3$, δ): 8.38 (bs, 2H), 4.20 (bs, 8H), 3.62 (bs, 8H), 3.36 (bs, 8H), 1.16-1.60 (m, 44H), 0.90-0.99 (m, 24H). GPC (THF, PS): M_n = 11,000 Đ = 2.03.

3.5 ICP-MS and NMR data for Relevant Compounds

Table 3.3. Elemental concentrations (ppm) for ECP-Magenta samples made via DHAP in various solvents. Table 3.3 continues onto page 54.

Element	NMP _BP	NMP _AP	DMAc_BP	DMAc_AP	HMPA_BP	HMPA_AP
Li	3.5	1.4	7.0	1.3	5.4	0.7
B	23.6	7.8	6.7	6.8	8.1	5.4
Na	82.2	17.9	98.1	37.9	844.8	566.3
Mg	7.49	9.75	bdl	56.08	9.83	48.93
Al	bdl	5.57	2.65	141.13	bdl	26.17
Si	401	1826	1072	15487	1446	13884
P	6.2	2.5	21.4	22.8	17764	88.3
K	1109	277	33694	442	25967	406
Ca	357.2	217.9	162.6	383.1	254.1	320.6
Sc	0.3	0.3	0.2	0.3	0.2	0.3
Ti	0.25	0.96	bdl	1.52	bdl	2.15
V	0.27	0.28	0.21	0.39	0.21	0.31
Cr	45.59	40.96	25.31	59.76	15.87	26.41
Mn	1.89	1.82	1.43	3.14	1.42	2.19
Fe	0.73	10.64	35.76	91.95	44.98	50.68
Co	0.10	0.12	0.10	0.33	0.15	0.19
Ni	1.21	2.37	6.42	6.09	6.43	4.02
Cu	3.35	1.82	7.36	3.23	6.65	2.09
Zn	36.24	14.53	42.44	10.99	1510	24.90
Ga	0.45	0.47	0.32	0.61	0.39	0.53
Ge	6.49	8.26	5.53	11.52	6.29	8.83
Rb	0.70	0.60	1.64	0.83	1.55	0.60
Sr	3.14	3.38	2.50	5.01	4.39	4.71
Y	0.43	0.47	0.30	1.12	0.36	0.76
Zr	0.45	0.61	0.30	0.75	0.55	0.58
Nb	0.17	0.18	0.12	0.23	0.16	0.18
Mo	bdl	0.12	bdl	bdl	bdl	bdl
Ru	0.01	0.00	0.01	0.02	0.03	0.01
Pd	756.0	9.3	1132.4	11.4	2924.6	528.4
Ag	5.3	4.0	2.7	4.9	3.1	4.2
Cd	0.7	0.4	0.2	0.4	0.3	0.4
In	0.26	0.26	0.17	0.33	0.21	0.28
Sn	4.13	2.10	1.64	3.36	2.32	2.97
Sb	bdl	bdl	bdl	bdl	bdl	bdl
Te	13.24	14.27	9.30	17.48	10.99	15.15
Cs	0.34	0.33	0.20	0.51	0.92	0.46
Ba	1.79	3.44	1.67	6.07	9.08	10.20
La	0.343	0.357	0.242	0.461	0.288	0.398
Ce	0.365	0.383	0.259	0.507	0.308	0.430
Pr	0.344	0.357	0.241	0.457	0.284	0.393
Nd	0.227	0.231	0.159	0.309	0.188	0.253
Sm	0.393	0.406	0.271	0.526	0.323	0.449
Eu	0.879	0.924	0.626	1.188	0.741	1.027
Gd	0.243	0.286	0.191	0.348	0.213	0.303
Tb	0.356	0.369	0.250	0.470	0.295	0.408
Dy	0.560	0.582	0.393	0.740	0.465	0.641
Ho	0.548	0.569	0.385	0.724	0.455	0.628
Er	0.588	0.610	0.413	0.776	0.488	0.673
Tm	0.442	0.459	0.310	0.583	0.367	0.506

bdl: below detection limit.

Yb	0.460	0.476	0.322	0.606	0.381	0.525
Lu	0.319	0.331	0.224	0.421	0.265	0.366
Hf	bdl	bdl	bdl	bdl	bdl	bdl
Ta	0.717	0.742	0.501	0.943	0.592	0.814
W	0.597	0.606	0.414	0.782	0.485	0.675
Ir	0.352	0.170	0.082	0.107	0.061	0.066
Pt	0.004	0.001	0.004	0.004	0.013	0.007
Au	0.054	0.010	0.020	0.012	0.003	0.003
Tl	bdl	bdl	bdl	bdl	bdl	bdl
Pb	bdl	bdl	bdl	bdl	bdl	bdl
Bi	0.495	0.568	0.323	1.240	0.379	0.535
Th	0.479	0.497	0.337	0.632	0.397	0.547
U	0.476	0.494	0.334	0.628	0.395	0.544

Table 3.4 Elemental concentrations (ppm) for various ECP samples made via DHAP in NMP after purification (AP). Table 3.4 continues onto page 55.

Element	Cyan_AP	Black_AP	Yellow_AP	Blue_AP
Li	35.6	79.9	39.7	45.9
B	63.6	165.6	74.0	107.6
Na	bdl	bdl	bdl	bdl
Mg	50.6	328.1	53.1	57.5
Al	89.5	241.8	99.1	118.3
Si	bdl	3294	272.6	738.1
P	5.5	23.4	-2.1	13.4
K	bdl	bdl	bdl	bdl
Ca	98.2	1322.9	413.7	385.3
Sc	bdl	bdl	bdl	bdl
Ti	21.9	52.8	23.8	30.3
V	bdl	bdl	bdl	bdl
Cr	34.2	71.7	38.0	42.9
Mn	51.7	113.3	59.5	69.3
Fe	48.5	107.5	69.4	56.6
Co	bdl	bdl	bdl	bdl
Ni	49.6	112.4	56.5	82.8
Cu	47.2	132.4	57.7	78.7
Zn	12.9	39.9	22.1	85.8
Ga	bdl	bdl	bdl	bdl
Ge	7.9	31.2	10.8	13.2
Rb	bdl	bdl	bdl	bdl
Sr	48.6	109.4	56.2	64.8
Y	bdl	bdl	bdl	bdl
Zr	bdl	bdl	bdl	bdl
Nb	bdl	bdl	bdl	bdl
Mo	17.0	36.5	19.1	22.2
Ru	bdl	0.2	bdl	bdl
Pd	214.59	118.68	216.29	230.22
Ag	61.16	133.42	69.42	80.21
Cd	39.39	86.09	44.51	51.91
In	bdl	bdl	bdl	bdl
Sn	4.71	19.99	29.67	21.26
Sb	bdl	bdl	bdl	bdl
Te	54.19	117.07	60.85	75.42
Cs	bdl	bdl	bdl	bdl
Ba	58.70	142.38	68.46	81.66
La	bdl	bdl	bdl	bdl
Ce	bdl	bdl	bdl	bdl
Pr	bdl	bdl	bdl	bdl
Nd	bdl	bdl	bdl	bdl
Sm	bdl	bdl	bdl	bdl
Eu	bdl	bdl	bdl	bdl
Gd	bdl	bdl	bdl	bdl
Tb	bdl	bdl	bdl	bdl
Dy	bdl	bdl	bdl	bdl
Ho	bdl	bdl	bdl	bdl
Er	bdl	bdl	bdl	bdl
Tm	bdl	bdl	bdl	bdl

Yb	bdl	bdl	bdl	bdl
Lu	bdl	bdl	bdl	bdl
Hf	bdl	bdl	bdl	bdl
Ta	bdl	bdl	bdl	bdl
W	bdl	bdl	bdl	bdl
Ir	0.14	0.40	0.06	0.06
Pt	0.16	0.00	0.03	0.05
Au	0.44	4.40	0.50	0.30
Tl	48.37	105.44	54.80	63.41
Pb	5.05	11.73	5.77	7.66
Bi	bdl	bdl	bdl	bdl
Th	bdl	bdl	bdl	bdl
U	bdl	bdl	bdl	bdl

bdl: below detection limit.

Table 3.5. Elemental concentrations (ppm) for various ECP samples made via DHAP in NMP after purification (AP).

Element	OxP	GRIM	DHAP (AP)	Element	OxP	GRIM	DHAP (AP)
Li	bdl	1.49	1.4	In	0.13	0.12	0.26
B	25.30	1.55	7.8	Sn	2.13	1.39	2.10
Na	bdl	bdl	17.9	Sb	bdl	bdl	bdl
Mg	37	1636	9.75	Te	10.87	10.57	14.27
Al	61	49	5.57	Cs	0.11	0.10	0.33
Si	641	533	1826	Ba	4.41	4.77	3.44
P	5.25	29.35	2.5	La	bdl	bdl	0.357
K	209	228	277.1	Ce	0.22	0.21	0.383
Ca	130	96	217.9	Pr	0.09	0.09	0.357
Sc	0.15	0.14	0.3	Nd	bdl	bdl	0.231
Ti	1.52	0.95	0.96	Sm	0.49	0.47	0.406
V	0.66	0.47	0.28	Eu	0.01	0.01	0.924
Cr	0.60	bdl	40.96	Gd	bdl	bdl	0.286
Mn	1.34	1.61	1.82	Tb	0.52	0.51	0.369
Fe	1112	6	10.64	Dy	0.11	0.11	0.582
Co	0.05	0.00	0.12	Ho	0.19	0.19	0.569
Ni	1.74	926	2.37	Er	bdl	bdl	0.610
Cu	4.60	0.05	1.82	Tm	0.26	0.25	0.459
Zn	63.1	8.4	14.53	Yb	bdl	bdl	0.476
Ga	0.24	0.17	0.47	Lu	0.03	0.03	0.331
Ge	12.7	7.7	8.26	Hf	0.67	0.65	bdl
Rb	0.32	0.31	0.60	Ta	bdl	bdl	0.742
Sr	0.94	0.74	3.38	W	bdl	bdl	0.606
Y	0.45	0.43	0.47	Re	0.58	0.57	Not obtained
Zr	0.11	0.07	0.61	Ir	0.03	0.00	0.170
Nb	0.25	0.02	0.18	Pt	11.83	11.50	0.001
Mo	bdl	bdl	0.12	Au	0.01	0.01	0.010
Ru	0.01	0.00	0.00	Tl	bdl	bdl	bdl
Rh	0.01	0.01	0.02	Pb	0.76	bdl	bdl
Pd	0.37	0.36	9.3	Bi	0.32	0.28	0.568
Ag	bdl	bdl	4.0	Th	0.16	0.15	0.497
Cd	0.50	0.43	0.4	U	0.36	0.35	0.494

bdl: below detection limit

^{1}H and ^{13}C NMR spectra of novel compounds.

6,8-dibromo-3,3-bis((2-ethylhexyloxy)methyl)-3,4-dihydro-2H-thieno[3,4-b][1,4]dioxepine (3)

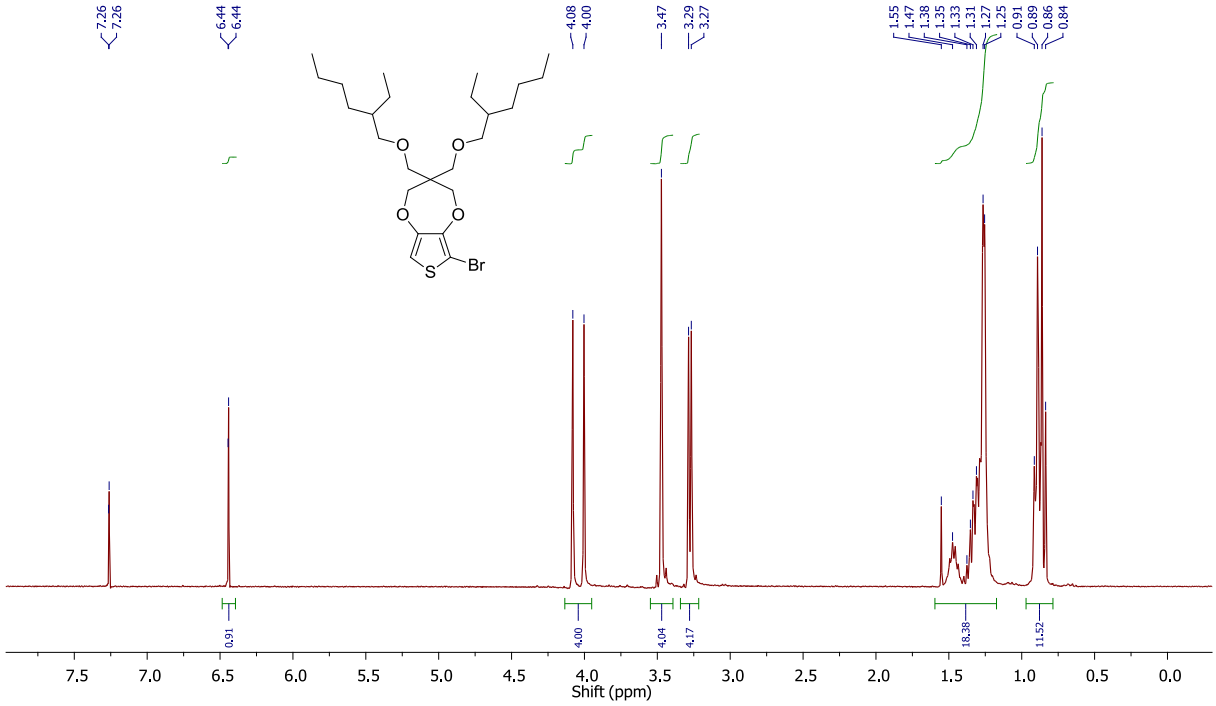

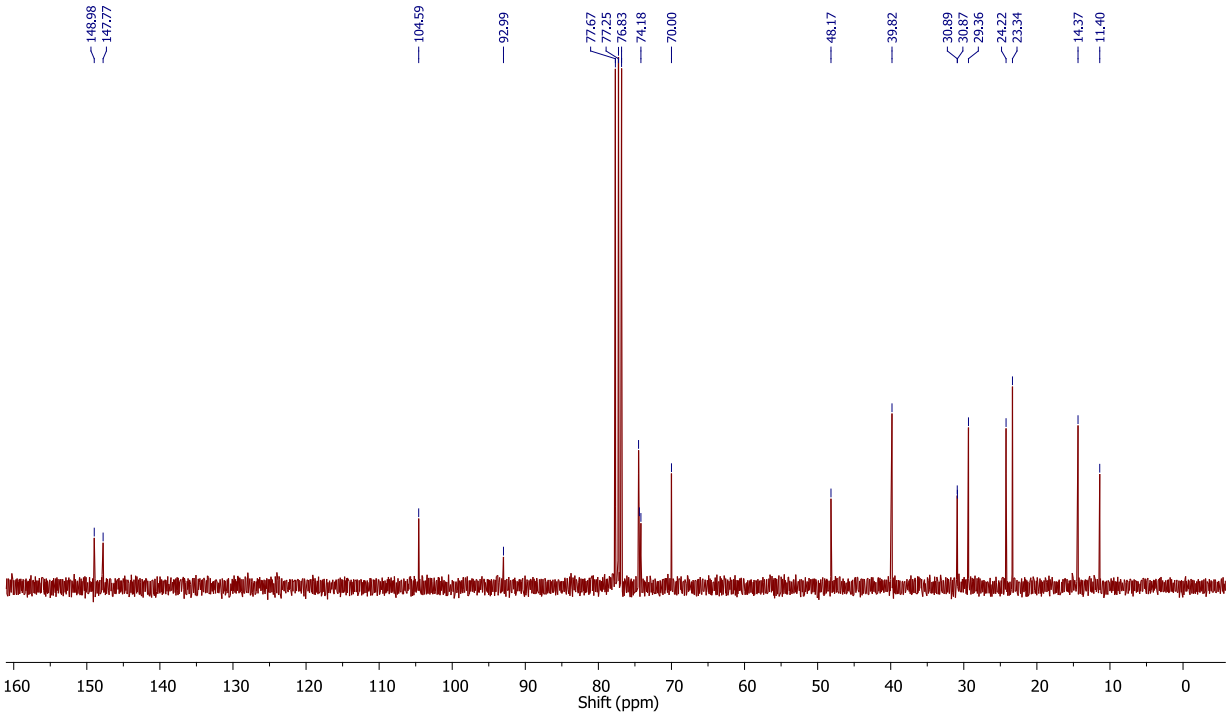

3,3,3',3'-tetrakis(((2-ethylhexyl)oxy)methyl)-3,3',4,4'-tetrahydro-2H,2'H-6,6'-bithieno[3,4 -b][1,4]dioxepine (6)

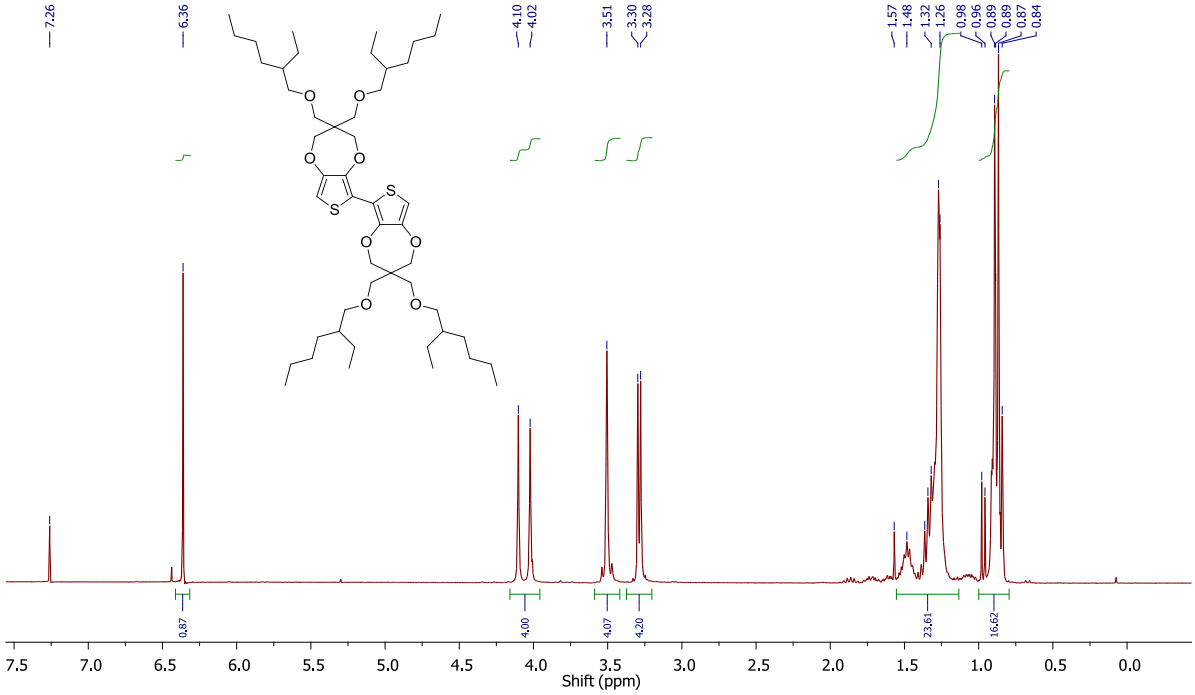

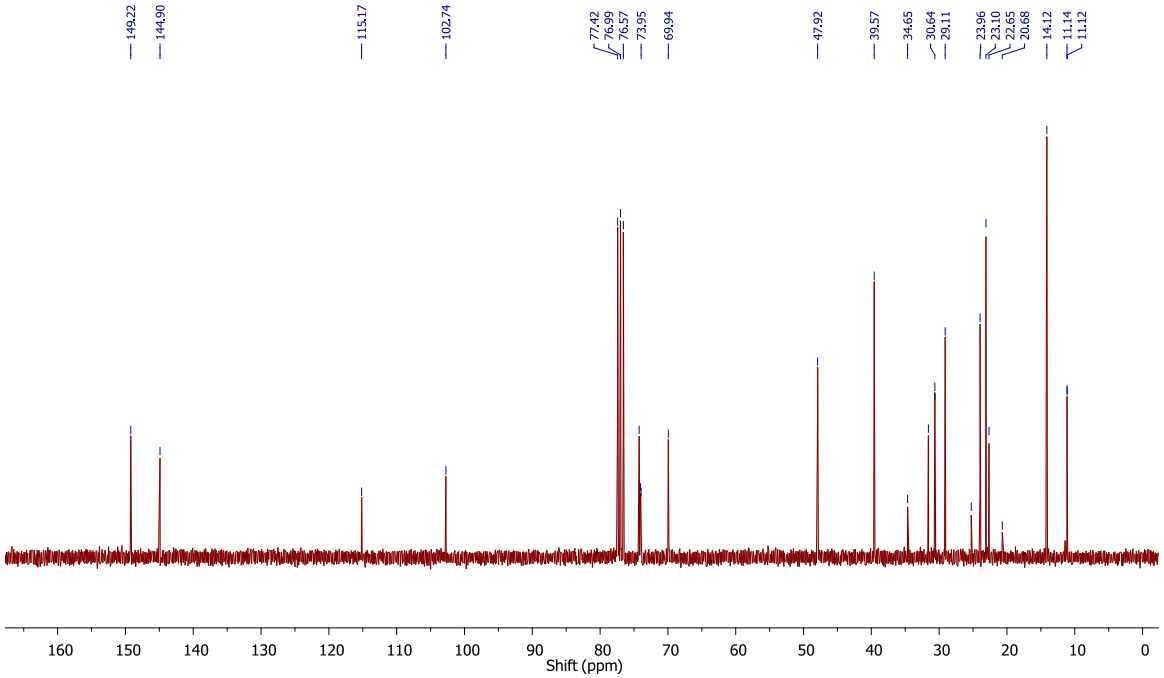

ECP-Magenta ^{1}H NMR

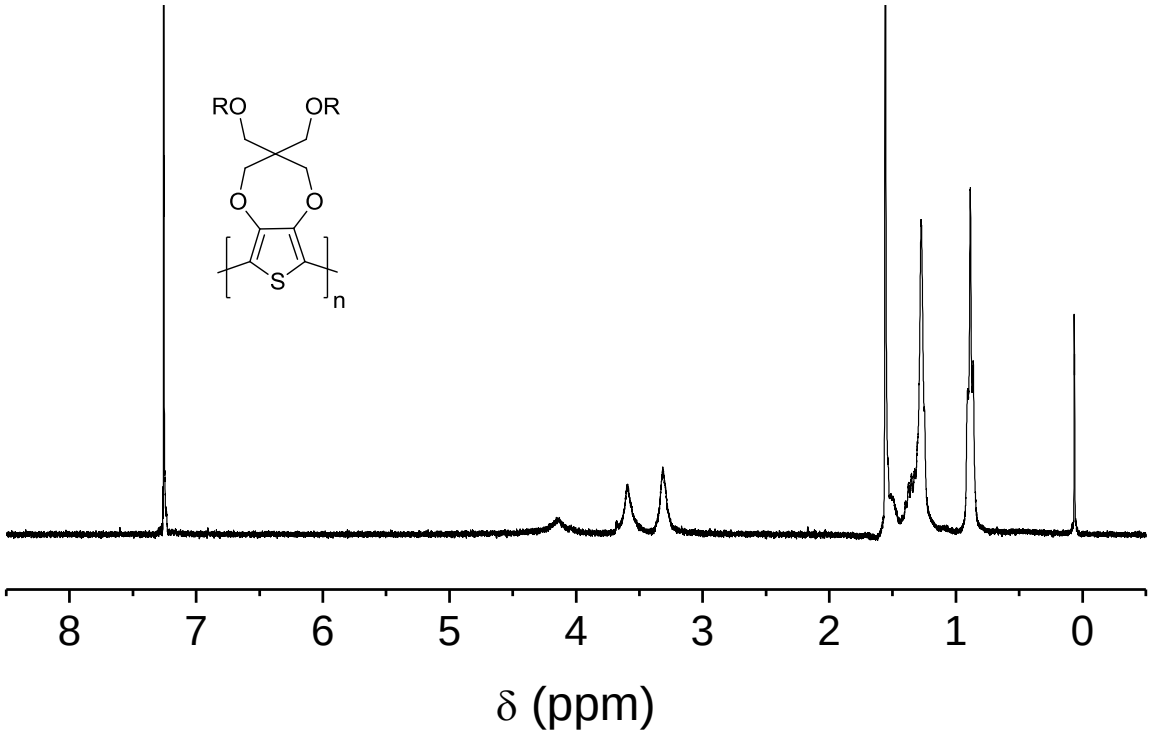

ECP-Blue ^{1}H NMR

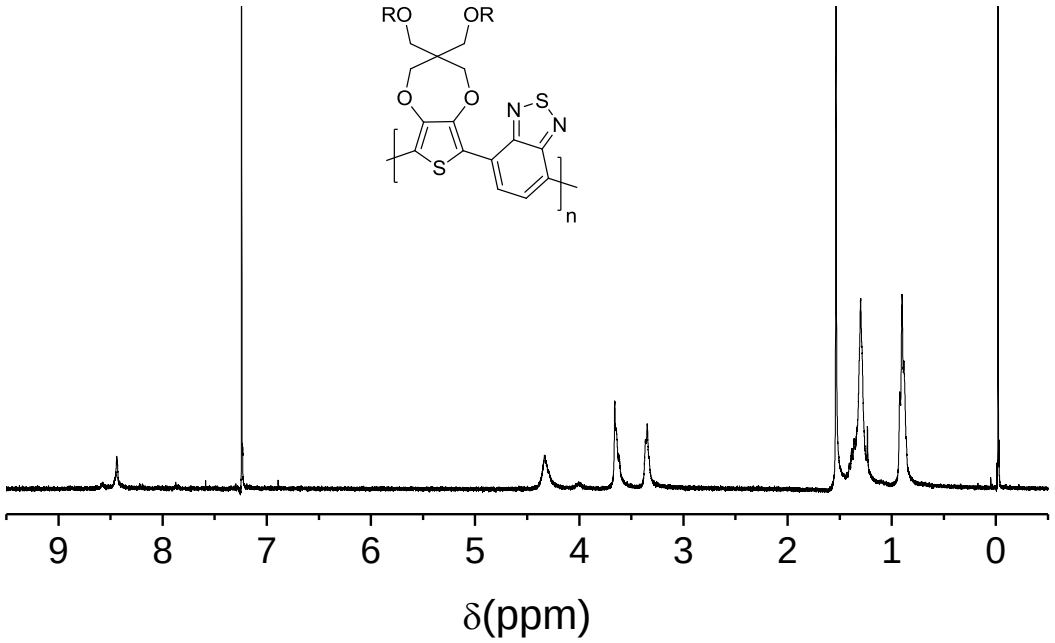

ECP-Cyan ^{1}H NMR

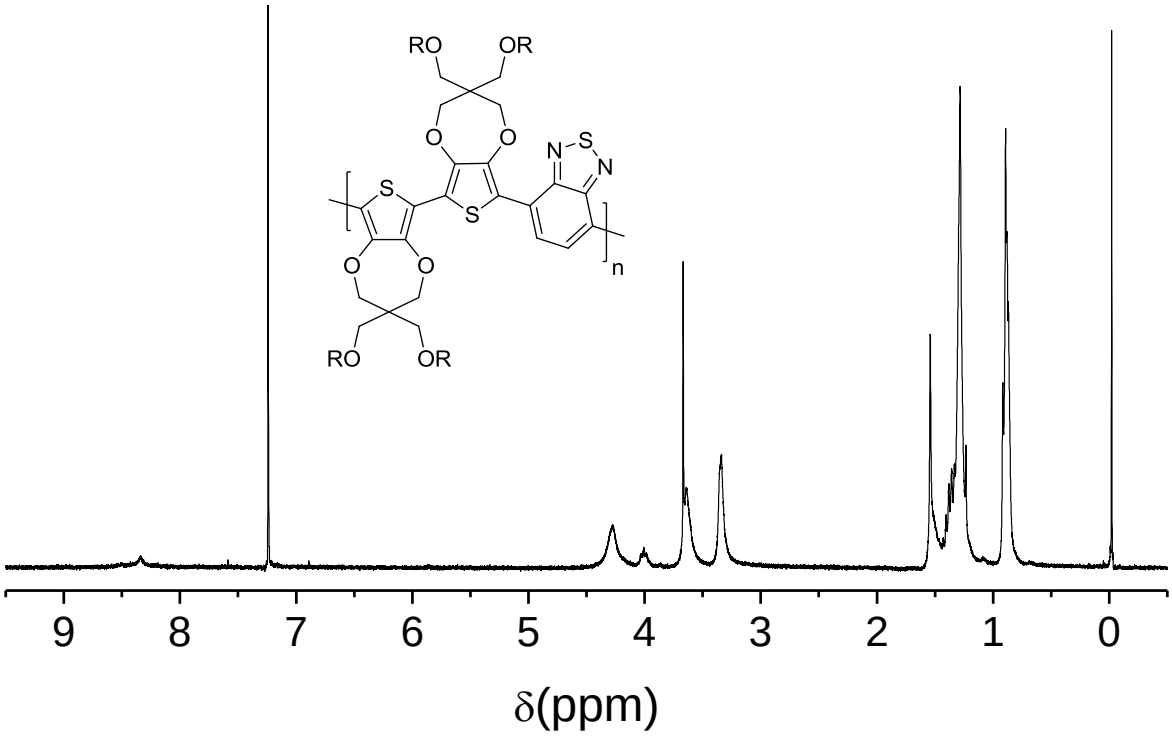

ECP-Yellow ^{1}H NMR

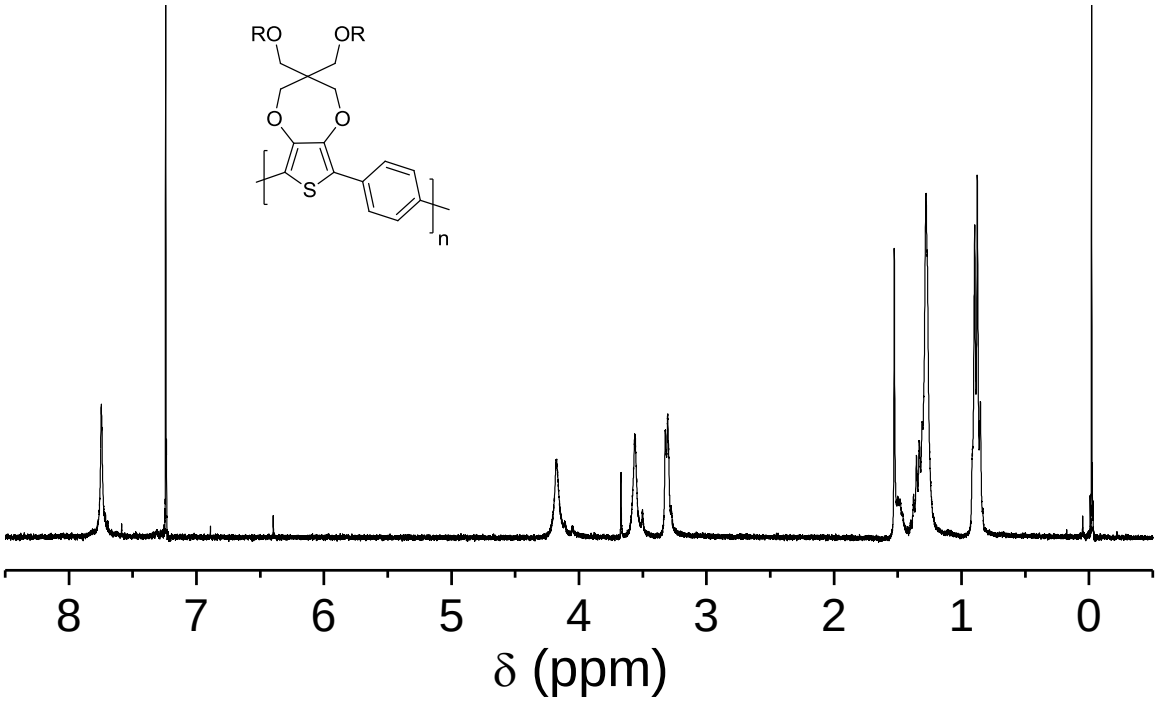

ECP-Black ^{1}H NMR

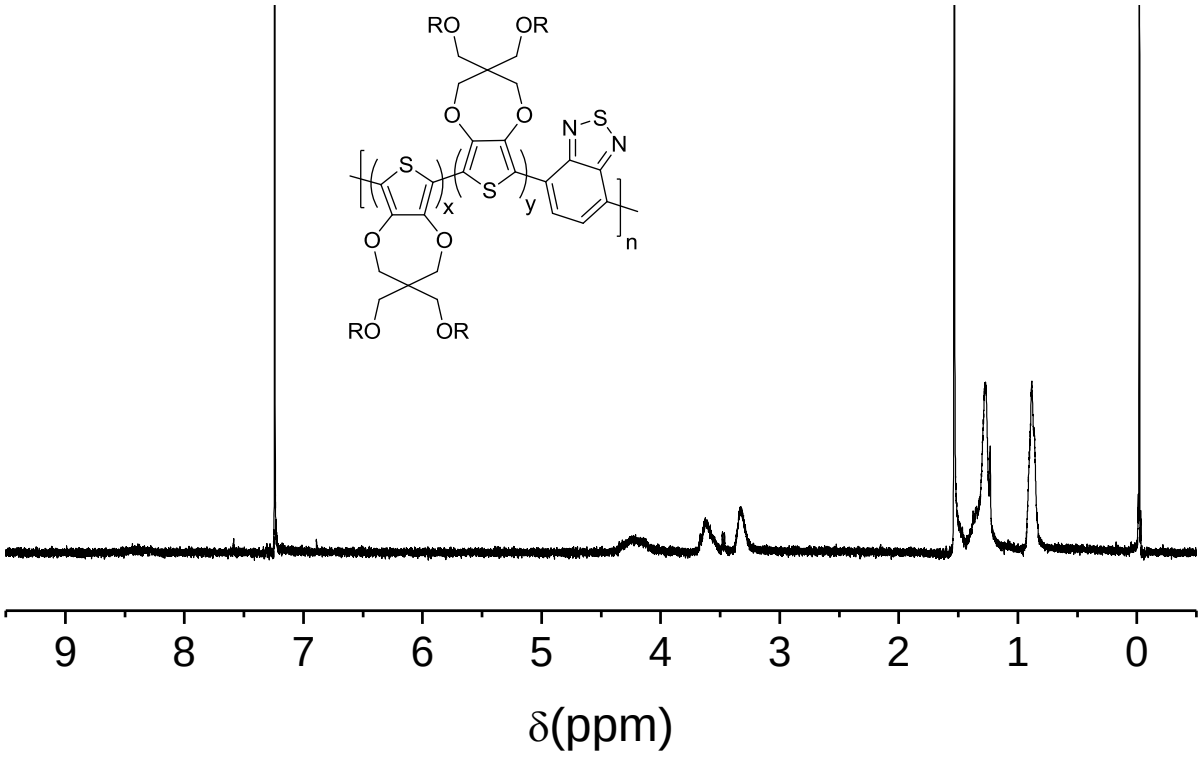

3.5 References

[1] Negishi, E. *Angew. Chem. Int. Ed.* **2011**, 50, 6738.

[2] Leclerc, M.; Morin, J.-F. *Design and Synthesis of Conjugated Polymers.* Wiley-VCH, Weinheim, **2010**.

[3] Arias, A. C.; MacKenzie, J. D.; McCulloch, I.; Rivnay, J.; Salleo, A. *Chem. Rev.* **2010**, 110, 3.

[4] DeVries, J. G. *Can. J. Chem.* **2001**, 79, 1086.

[5] Ullmann, F.; Bielecki, J. *Ber. Dtsch. Chem. Ges.* **1901**, 34, 2174.

[6] Goldberg, I. *Ber. Dtsch. Chem. Ges.* **1906**, 39, 1691.

[7] Ackermann, L.; Vicente, R.; Kapdi, A. P. *Angew. Chem. Int. Ed.* **2009**, 48, 9792.

[8] Gorelsky, S.; Lapointe, D.; Fagnou, K. *J. Org. Chem.* **2012**, 77, 658.

[9] Lapointe, D.; Fagnou, K. *Chem. Lett.* **2010**, 39, 1118.

[10] Kuhl, N.; Hopkinson, M. N.; Wencel-Delord, J.; Glorius, F. *Angew. Chem. Int. Ed.* **2012**, 51, 10236.

[11] Gorelsky, S. I. Coord. *Chem. Rev.* **2013**, 257, 153.

[12] Schipper, D. J.; Fagnou, K. *Chem. Mater.* **2011**, 23, 1594.

[13] Liégault, B.; Lapointe, D.; Caron, L.; Vlassova, A.; Fagnou, K. *J. Org. Chem.* **2009**, 74, 1826.

[14] Tan, Y; Hartwig, J. F. *J. Am. Chem. Soc.* **2011**, 133, 3308.

[15] Fujinami, Y.; Kuwabara, J.; Lu, W.; Hayashi, H.; Kanbara, T. *ACS Macro. Lett.* **2012**, 1, 67.

[16] Lu, W.; Kuwabara, J.; Kanbara, T. *Polym. Chem.* **2012**, 3, 3217.

[17] Kowalski, S.; Allard, S.; Scherf, U. *ACS Macro. Lett.* **2012**, 1, 465.

[18] Rudenko, A. E.; Wiley, C. A.; Stone, S. M.; Tannaci, J. F.; Thompson, B. C. J. Polym. Sci. A: *Polym. Chem.* **2012**, 50, 3691.

[19] Zhao, H.; Liu, C.-Y.; Luo, S.-C.; Zhu, B.; Wang, T.-H.; Hsu, H.-S.; Yu, H.-H. *Macromolecules* **2012**, 45, 7783.

[20] Chang, S.-W.; Waters, H.; Kettle, J.; Kuo, Z.-R.; Li, C.-H.; Yu, C.-Y.; Horie, M. *Macromol. Rapid Commun.* **2012**, 33, 1927.

[21] Kuwabara, J.; Nohara, Y.; Choi, S. J.; Fujinami, Y.; Lu, W.; Yo-shimura, K.; Oguma, J.; Suenobu, K.; Kanbara, T. *Polym. Chem*. **2013**, 4, 947.

[22] Yamazaki, K.; Kuwabara, J.; Kanbara, T. *Macromol. Rapid. Commun.* **2013**, 34, 69.

[23] Sinha, J.; Lee, S. J.; Kong, H.; Swift, T. W.; Katz, H. E. *Macromolecules* **2013**,

[24] Adachi, T.; Tong, L.; Kuwabara, J.; Kanbara, T.; Saeki, A.; Seki, S.; Yamamoto, Y. *J. Am. Chem. Soc.* **2013**, 135, 870.

[25] Current methods for polymer purification include precipitation in a non-solvent, filtration, redissolution and treatment with chelating/neutralizing agents, reprecipitation, and finally Soxhlet extraction. Each step introduces metal/non-metal contaminants that affect the overall purity of the polymer, plus the time and materials cost. As an example of this see: Chen, T.-A.; Wu, X.; Rieke, R. D. *J. Am. Chem. Soc.* **1995**, 117, 233.

[26] Goodson, F. E.; Wallow, T. I.; Novak, B. M. *Macromolecules* **1998**, 31, 2047.

[27] Goodson, F. E.; Hauck, S. I.; Hartwig, J. F. *J. Am. Chem. Soc.* **1999**, 121, 7527.

[28] Abdou, M. S. A.; Lu, X.; Xie, Z. W.; Orfino, F.; Deen, M. J.; Holdcroft, S. *Chem. Mater.* **1995**, 7, 631.

[29] Lupton, J. M.; Pogantsch, A.; Piok, T.; List, E. J. W.; Patil, S.; Scherf, U. *Phys. Rev. Lett.* **2002**, 89, 167401.

[30] Cugola, R.; Giovanella, U.; Di Giancincenzo, P.; Bertini, F.; Catellani, M.; Luzzati, S. *Thin Solid Films* **2006**, 511-512, 489.

[31] Colladet, K.; Fourier, S.; Cleij, T. J.; Lutsen, L.; Gelan, J; Vanderzande, D.; Nguyen, L. H.; Neugebauer, H.; Sariciftci, S.; Aguirre, A.; Janssen, G.; Goovaerts, E. *Macromol-ecules* **2007**, 40, 65.

[32] Kaake, L. G.; Barbara, P. F.; Zhu, X.-Y. J. *Phys. Chem. Lett.* **2010**, 1, 628.

[33] Kaake, L.; Dang, X.-D.; Leong, W.-L.; Zhang, Y.; Heeger, A.; Nguyen, T.-Q. *Adv. Mater.* **2013**.

[34] Dyer, A. L.; Thompson, E. J.; Reynolds, J. R. *ACS Appl. Mater. Interfaces* **2011**, 3, 1787.

[35] Amb, C. M.; Dyer, A. L.; Reynolds, J. R. *Chem. Mater.* **2011**, 23, 397.

[36] Reeves, B. D.; Unur, E.; Ananthakrishnan, N.; Reynolds, J. R. *Macromolecules* **2007**, 40, 5344.

[37] Kumar, A.; Singh, R.; Go-pinathan, S. P.; Kumar, A. *Chem. Commun.* **2012**, 48, 4905.

[38] Reeves, B. D.; Grenier, C. R. G.; Argun, A. A.; Cirpan, A.; McCarley, T. D.; Reynolds, J. R. *Macromolecules* **2004**, 37, 7559.

[39] Grenier, C. R. G.; George, S. J.; Joncheray, T. J.; Meijer, E. W.; Reynolds, J. R. *J. Am. Chem. Soc.* **2007**, 129, 10694.

[40] Gilbert, R. G.; Hess, M.; Jenkins, A. D.; Jones, R. G.; Kratochvíl, P.; Stepto, R. F. T. *Pure Appl. Chem*. **2009**, 81, 351.

[41] As examples of chain-growth polymerizations with conjugated materials see: (a) Yokoyama, A.; Suzuki, H.; Kubota, Y.; Ohnuchi, K.; Higashimura, H.; Yokozawa, T. *J. Am. Chem. Soc.* **2007**, 129, 7236. (b) Zhang, H.-H.; Xing, C.-H.; Hu, Q.-S. *J. Am. Chem. Soc.* **2012**, 134, 13156.

[42] Wang, Q.; Wakioka, M.; Ozawa, F. *Macromol. Rapid Commun.* **2012**, 33, 1203.

[43] Turro, N. J. *Modern Molecular Photochemistry*. University Science Books, Sausalito, CA, **1991**.

[44] Amb, C. M.; Beaujuge, P. M.; Reynolds, J. R. *Adv. Mater.* 2010, 22, 724.

[45] Beaujuge, P. M.; Vasilyeva, S. V.; Ellinger, S.; McCarley, T. D.; Reynolds, J. R. *Macromolecules* **2009**, 42, 3694.

[46] Amb, C. M.; Kerszulis, J. A.; Thompson, E. J.; Dyer, A. L.; Reynolds, J. R. *Polym. Chem.* **2011**, 2, 812.

[47] Shi, P.; Amb, C. M.; Knott, E. P.; Thompson, E. J.; Liu, D. Y.; Mei, J.; Dyer, A. L.; Reynolds, A. L. *Adv. Mater.* **2010**, 22, 4949. Dfds

CHAPTER 4

CONCLUSION

4.1 Outlook of Research

Research in the field of conjugated polymers has only continued to grow as illustrated by the steady yearly increase in peer reviewed publications. One reason for this trend is due to conjugated polymers use in systems that have the potential to significantly change our daily lives for the better (OLEDs, OFETs, NLOs, OECs).

Furthermore, the work described in this thesis has shown new synthetic methodology that provides the ability to access a wide range of novel monomers and polymers, and additionally improve on the overall synthesis of well-defined polymeric systems.

As mentioned previously, the ability to access long alkyl chains, or variously functionalized DTGs, opens up new possibilities for synthesizing previously difficult to prepare donor materials for the organic electronic fields of OPV and OFETs. Finally, the use of DHAP as a route to previously synthetized electrochromic polymers provides a methodology that provides lower atom economy, shorter reaction times, and simpler purification methods that can significantly reduce costs for the production of electrochromic based systems and products.